Dynamic Interference Management for UAV-Assisted Wireless Networks

Ali Rahmati[®], *Member, IEEE*, Seyyedali Hosseinalipour[®], *Member, IEEE*,
Yavuz Yapıcı[®], *Senior Member, IEEE*, Xiaofan He[®], *Member, IEEE*, Ismail Güvenç[®], *Fellow, IEEE*,
Huaiyu Dai[®], *Fellow, IEEE*, and Arupjyoti Bhuyan[®], *Senior Member, IEEE*

Abstract—We investigate a transmission mechanism aiming to improve the data rate between a base station (BS) and a user equipment (UE) through deploying multiple relaying UAVs. We consider the effect of interference incurred by another established communication network, which makes our problem challenging and different from the state of the art. We aim to design the 3D trajectories and power allocation for the UAVs to maximize the data flow of the network while keeping the interference on the existing communication network below a threshold. We utilize the mobility feature of the UAVs to evade the (un)-intended interference caused by (un)-intentional interferers. To this end, we propose an alternating-maximization approach to jointly obtain the 3D trajectories and the UAVs transmission powers. We handle the 3D trajectory design by resorting to spectral graph theory and subsequently address the power allocation through convex optimization techniques. We also approach the problem from the intentional interferer's perspective where smart jammers chase the UAVs to effectively degrade the data flow of the network. We also extend our work to the case for multiple UEs. Finally, we demonstrate the efficacy of our proposed method through extensive simulations.

Index Terms—Unmanned aerial vehicle (UAV), jammer, trajectory optimization, power allocation, interference management, smart interferer, spectral graph theory, Cheeger constant.

Manuscript received August 7, 2020; revised March 8, 2021 and July 5, 2021; accepted September 7, 2021. Date of publication September 28, 2021; date of current version April 11, 2022. This work was supported in part by Idaho National Laboratory (INL) Laboratory Directed Research and Development (LDRD) Program through Department of Energy (DoE) Idaho Operations Office under Contract DE-AC07-05ID14517 and in part by the U.S. National Science Foundation under Grant ECCS-1444009, Grant CNS-1824518, and Grant CNS-1910153. This article was presented in part at 2019 IEEE Globecom [DOI: 10.1109/GLOBECOM38437.2019.9013532]. The associate editor coordinating the review of this article and approving it for publication was L. Musavian. (Corresponding author: Huaiyu Dai.)

Ali Rahmati was with the Department of Electrical and Computer Engineering, NC State University, Raleigh, NC 27695 USA. He is now with Qualcomm, Inc., San Diego, CA 92121 USA (e-mail: arahmat@ncsu.edu).

Seyyedali Hosseinalipour is with the School of Electrical and Computer Engineering, Purdue University, West Lafayette, IN 47907 USA (e-mail: hosseina@purdue.edu).

Yavuz Yapıcı was with the Department of Electrical Engineering, University of South Carolina, Columbia, SC 29201 USA. He is now with Qualcomm, Bridgewater Township, NJ 08807 USA (e-mail: yyapici@qti.qualcomm.com). Xiaofan He is with the School of Electronic Information, Wuhan University,

Xiaofan He is with the School of Electronic Information, Wuhan University Wuhan 430072, China (e-mail: xiaofanhe@whu.edu.cn).

Ismail Güvenç and Huaiyu Dai are with the Department of Electrical and Computer Engineering, North Carolina State University, Raleigh, NC 27695 USA (e-mail: iguvenc@ncsu.edu; hdai@ncsu.edu).

Arupjyoti Bhuyan is with Idaho National Laboratory, Idaho Falls, ID 83415 USA (e-mail: arupjyoti.bhuyan@inl.gov).

Color versions of one or more figures in this article are available at https://doi.org/10.1109/TWC.2021.3114234.

Digital Object Identifier 10.1109/TWC.2021.3114234

I. INTRODUCTION

THE utilization of unmanned aerial vehicles (UAVs) has recently become a practical approach for a variety of mission-driven applications including border surveillance, natural disasters aftermath, monitoring, search and rescue, and purchase delivery [2]-[4]. Owing to the low acquisition cost of UAVs as well as their fast deployment and efficient coverage capabilities, UAV-assisted wireless communications has recently attracted extensive interest [5], [6]. Specifically, the 3D mobility feature of UAVs and the coexistence of relaying UAVs with other existing communication networks (e.g., cellular networks) have led to new design challenges and opportunities in these networks [7], [8], which are not investigated in the context of classic wireless sensor networks [9]. This fact has promoted an extensive literature dedicated to studying the unique design aspects of these networks, e.g., [10]-[20]. In current literature, the UAV-assisted relay communication is mainly studied in two different contexts, in which the network is assumed to be either static, i.e., the positions of the UAVs, transmitters, and receivers are fixed during the data transmission [10]–[14], [21], [22], or dynamic [15]–[20], where the positions of the transmitters and receivers are assumed to be fixed while the UAVs are typically assumed to be mobile.

In the context of static UAV-assisted wireless communications, in [21], considering an interference limited in band downlink cellular network, the authors studied the effects of scheduling criteria, mobility constraints, path loss models, backhaul constraints, and 3D antenna radiation pattern on the trajectory optimization of a UAV. In [10], the optimal deployment of a UAV in a wireless relay communication system is studied in order to improve the quality of communications between two obstructed access points by maximizing the average data rate of the system, while keeping the symbol error rate below a threshold. In [11], a relay network is considered in the context of a four node channel setup consisting of a transmitter, a receiver, a UAV relay, and an eavesdropper, where the goal is to shed light on the application of UAV-enabled relaying in secure wireless communications. In [12], the UAVs are utilized to form an aerial backhaul network to enhance the performance of the ground network, which is measured through data rate and delay. The link configuration between the UAVs and the gateways, and among

1536-1276 © 2021 IEEE. Personal use is permitted, but republication/redistribution requires IEEE permission. See https://www.ieee.org/publications/rights/index.html for more information.

the UAVs, is formulated as a network formation game, which is solved through a myopic network formation algorithm. The optimal locations of the UAV are derived in [13] through maximizing the data rate in single link multi-hop and multiple links dual-hop relaying schemes. In this work, it is assumed that the UAVs are hovering at an identical fixed altitude during the transmission. As a follow-up work for [13], in our recent works [14], [22], we studied the optimal position planning of UAV relays, which coexist with a major interferer in the environment. In these works, we investigated the following two new problems: i) identifying the minimum required number of UAVs and their optimal positions to satisfy a given SIR of the system, ii) developing a distributed algorithm to maximize the SIR of the system requiring message exchange only between adjacent UAV relays.

In the context of dynamic UAV-assisted wireless communication, in [15], the joint optimization of propulsion and transmission energies for a UAV relay-assisted communication network is studied. An optimal control problem is formulated for energy minimization based on dynamic models for both transmission and mobility. In [16], the optimal altitude of a UAV for both static and mobile relaying, which corresponds to the circular movements around the user, is considered to maximize the reliability of the system, which is measured through total power loss, the overall outage, and the overall bit error rate. It is shown that that decode-and-forward relaying is better than amplify-and-forward relaying in terms of reliability. In [17], a UAV-assisted relay communication network is proposed, where the UAV serves as a relay between a base station and a mobile device. The amplify-and-forward relaying scheme is used, for which the trajectory of UAV, the transmit power of both the UAV and the mobile device are obtained to minimize the outage probability of the system. In [18], assuming a source-destination pair and a UAV relay, an end-to-end throughput maximization problem is formulated to optimize the relay trajectory and the source/relay power allocations subject to practical constraints on the UAV speed, transmitting power of the transmitter and the UAV, etc. Afterward, an alternating optimization approach is proposed to jointly derive the optimal transmission power of the transmitter and the UAV, and the UAV trajectory. In [19], a wireless relay network model is considered, in which a fixed-wing UAV serves as a relay among the ground stations with disconnected communication links in the event of disasters. It is assumed that the UAV deploys the decode-and-forward relaying protocol. Considering the fact that in contrast to rotatory-wing UAVs, fixedwing UAVs require circular movements to maintain their altitude, it is shown that the conventional fixed rate relaying will no longer be effective. To this end, a variable rate relaying approach is proposed to enhance the performance of the system measured through outage probability and information rate. In [20], UAVs are deployed in a wireless network in order to provide connectivity or boost the capacity for the ground users. A nested segmented propagation model is proposed for the air-to-ground channel, based on which they proposed an algorithm to search the optimal UAV position for establishing the best wireless relay link between a base station and a user in a dense urban area. In [30], a caching UAV-assisted

secure transmission scheme is proposed in hyper-dense smallcell networks based on interference alignment. The UAVs are utilized to provide data traffic to mobile users cooperatively with small cell base stations. In [31], multi-hop D2D communication is leveraged to extend the coverage of UAVs effectively in order to perform emergency transmission for IoT in disasters. Two optimal transceiver design schemes are proposed for the uplink and the downlink, respectively, to improve the performance of UAV transmission. In [32], the authors considered a single-cell multi-UAV network, where multiple UAVs upload their collected data to the BS. They introduced a cooperative UAV sense-and-send protocol in which a sub-channel allocation and UAV speed optimization problem is formulated to increase the uplink sum-rate of the network. Authors in [33] considered a dynamic fly-hovertransmit scheme for the UAV-aided efficient wireless information transfer in a cognitive radio network. They deployed the Markov decision process to solve the UAV's expected sum-throughput maximization problem with considering the battery levels of the UAVs. In [34], a highly reliable and low latency communication for a cellular-connected UAV swarm is introduced in which they take advantage of D2D communication for the UAV swarm to improve the spectral and energy efficiency.

We have also conducted a comprehensive literature survey on joint power and trajectory optimization for UAV relays, and made a detailed comparison with the representative works of the current art as shown in Table I. As can be seen, about half of these works only consider single UAV relay, and only a few pursues trajectory design in the 3D space. More importantly, most of them do not consider the impact of interference; among the few works that consider interference and jamming (including one of our recent works), only single interferer is explored, the trajectory design is limited to 1D/2D, and simplified communication scenarios (single relay or no power control) are considered. In contrast, our proposed approach is general enough to consider all these scenarios in itself.

In this work, we consider the application of UAV relays for a more complicated relay network structure, where the network consists of multiple ground/terrestrial nodes and aerial nodes, i.e., UAVs. The direction for the flow of information is assumed to be time varying and thus unknown a priori. In this context, all the UAVs and the ground nodes are considered to be a transceivers. We aim to propose a framework to enhance the current literature on the subject by incorporating the existence of interferers. To this end, we utilize the mobility of UAVs to avoid/suppress the interference from multiple interferers. For many emerging UAV applications, it is expected that the UAV network will need to co-exist with existing communication networks, such as cellular networks. This type of interference is mainly caused by the transmitters within the existing network, and hence is unintentional. In contrast, intentional interference coming from the jammers can happen both in civil and military applications. In this case, the legitimate UAVs are the relaying UAVs aiming to form a link between the BS and the UE, while the UAV jammers are assumed as adversary. The existence of multiple interferers in the 3D

environment makes our methodology different from the current literature. We pursue two different design schemes for two different types of interferers: (i) Unintentional interferer and (ii) Smart interferer. Unintentional interferers can be assumed as primary transmitters in the context of cognitive radio networks that produce interference unintentionally. In this case, we study the problem considering two scenarios. First, we assume that the UAV network and the co-existing network (which is referred to as the primary network) can cooperate to mitigate the mutual interference. Second, these two networks are assumed to be non-cooperative. We consider both the interference from the primary network to the UAV network and vice versa. Smart interferers, on the other hand, intentionally generate interference to interrupt or degrade the communication quality of the UAV network, e.g., mobile jammers or UAV users. Here, we consider the problem from the perspective of both the UAV network and the smart jammers. For the UAV network, we pursue the problem of joint power allocation and 3D trajectory design for UAVs to maximize the achievable data rate of the network. Also, for the smart jammers, we obtain the 3D trajectories with the goal to chase the UAV relays.

A. Summary of Contributions

- We investigate the UAV-assisted relay communication problem when the UAV network and another co-existing network cause interference on one another. We formulate the UAV trajectory design and power allocation as a single commodity maximum flow problem aiming to maximize the transmission flow of the network. We also take one step further and extend our work to the multiple UE setting. We consider a safety separation constraint for the UAVs to guarantee a proper flight in the 3D trajectory design. We address the problem considering two types of interferers: (i) Unintentional interferer and (ii) Smart interferer.
- Assuming an unintentional interferer, we address the 3D trajectory design and power allocation scheme while keeping the interference to the co-existing network below a pre-defined threshold. To this end, a solution for the 3D trajectory design is proposed resorting to spectral graph theory, in which the Cheeger constant is deployed. In addition, the power allocation design is achieved through the successive convex approximation (SCA) approach.
- Upon having smart interferers, we approach the problem from both the UAV network and the smart interferers' perspectives. We propose a 3D trajectory design for both the legitimate UAVs and the smart interferers. In this case, the legitimate UAVs aim to move towards a direction to evade the interference caused by the smart interferers. On the other hand, the smart UAV jammers aim to chase the legitimate UAVs to increase the interference intentionally and effectively degrade the communication flow between the BS and the user equipment (UE).

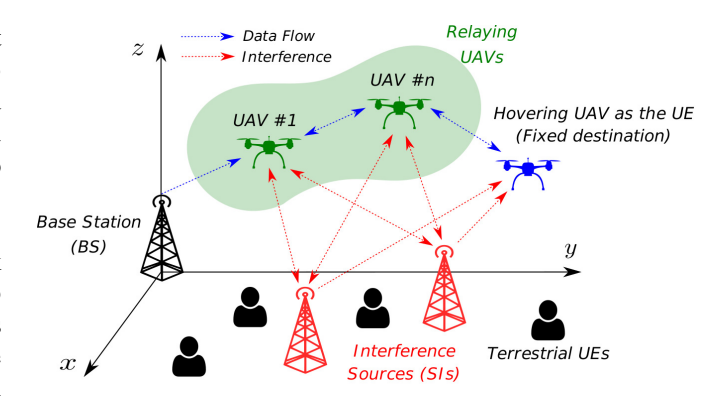


Fig. 1. System model for the communications scenario where the desired UE is also a flying UAV. The interferers are assumed as unintentional fixed interferers.

The rest of the paper is organized as follows. In Section II, the system model is presented. In Section III, the joint power allocation and 3D trajectory design is formulated and solved for unintentional interferer. Section IV presents the formulation and the solution of the maximum flow problem for the case of smart interferers. We have extended our scenario to consider multiple UEs in Section V. Simulation results are presented in Section VI and finally Section VII concludes the paper.

II. SYSTEM MODEL

In this section, we describe the communications scenario and the channel models for the air-to-air (A2A) and air-to-ground (A2G) links.

A. Communications Scenario

We consider a scenario where a terrestrial BS and a UE aim to engage in communication. The UE is either on the ground (e.g., a moving vehicle or pedestrian) or in the air (e.g., a UAV), as shown in Fig. 1. The channel condition of the direct link between the BS and the UE is not satisfactory for acceptable communication performance due to obstacles located in the line of sight (LoS) area or large distance [35]. To improve the data rate, we consider employing multiple UAVs relaying the signal between the BS and the UE. We also take into account the interference caused by the existing network (e.g., neighboring BSs, small cells, or jammers) on the UAV network, and describe the corresponding transmitters as interferers. We term the existing network as the primary network and its UEs as primary UEs. We assume that the interferers can be detected together with their transmission parameters using the existing sensing methods in the literature (e.g., [36]). Moreover, we assume that the BS, the UE, the UAVs and the interferers are functioning as both transmitters and receivers, i.e., transceivers, and thus can involve in both uplink and downlink of their own networks. In addition to the communication-related applications, another use case for this scenario is the aerial wireless sensor networks comprised of UAVs equipped with sensors and radio devices flying over an area of interest to sense and collect data.

We adopt time-division multiple access (TDMA) to schedule the relaying UAVs so that their transmissions do not collide

¹Throughout the paper, the smart interferer, the intended interferer, and intentional interferer terms may be used interchangeably.

Ref.	Goal	Single/Multi-hop	Power	Trajectory	Interferer	Implementation
[13]	Maximizing E2E SNR	Multi-hop	Х	2D	Х	Centralized
[14]	Minimum SIR maximization	Multi-hop	Х	1D	√(Single)	Centralized
[18]	Throughput maximization	Single-hop	\checkmark	2D	X	Centralized
[23]	Power minimization	Single-hop	\checkmark	2D	X	Centralized
[17]	Outage probability minimization	Single-hop	✓	3D	X	Centralized
[24]	Maximizing the E2E throughput	Multi-hop	✓	2D	×	Centralized
[25]	Maximizing the minimum rate	Single-hop	✓	2D	×	Centralized
[26]	Maximizing the E2E throughput	Multi-hop	✓	2D	×	Centralized
[27]	Maximizing sum rate	Single-hop	✓	3D	X	Centralized
[28]	Maximizing the min. average rate	Single-hop	✓	2D	X	Centralized
[29]	Maximizing the SNR	Single-hop	X	2D	$\sqrt{\text{(Single)}}$	Centralized
Ours	E2E throughput optimization	Multi-hop	✓	3D	√(Multiple)	Centralized/Distributed

TABLE I

COMPARISON OF THE PROPOSED WORK WITH RELEVANT LITERATURE ON UAV RELAY NETWORKS

with each other. Our goal is to obtain the 3D trajectories of the relaying UAVs along with the transmission powers to maximize the data rate between the BS and the UE, while the interference constraint on the primary network is met. As we consider a dynamic network, i.e., the nodes can move, designing 3D trajectories is critical since the UAVs should adaptively reconfigure their locations to avoid the interference and transmit their information simultaneously, more than just seeking the final locations to stop and transmit their information. It is worth noting that 3D trajectory design alone cannot guarantee that the interference threshold constraint is met for the primary network. Thus, a joint 3D trajectory design and power allocation is necessary to address such challenges.

In our setting, \mathcal{N} describes the set of N nodes in the network, which consists of the terrestrial BS (denoted by node s), the desired UE (denoted by node d), and the relaying UAVs. In addition, \mathcal{M} stands for the set of M interferers. The location of node $i \in \mathcal{N}$ in the UAV network is denoted by $\mathbf{r}_i = (x_i, y_i, z_i) \in \mathbb{R}^3$ such that $i \in \mathcal{N}$. Also, for the interferer nodes, we have $\mathbf{r}_{m}^{J} = (x_{m}^{J}, y_{m}^{J}, z_{m}^{J}) \in \mathbb{R}^3$, where $m \in \mathcal{M}$.

B. A2A and A2G Channel Models

In this section, we discuss the air-to-air (A2A) and the air-to-ground (A2G) channel models under consideration. The link between two UAVs (i.e., A2A channel) is modeled using the LoS model. To model the link between a UAV and the ground nodes (i.e., A2G and G2A channels) a weighted average between the LoS model and the NLoS model is used. In particular, the path-loss between the nodes i and j is defined as [37], [38]:

$$L_{i,j} = \begin{cases} (K_o d_{i,j})^{\alpha} \mu_{\text{LoS}}, & \text{if LoS link,} \\ (K_o d_{i,j})^{\alpha} \mu_{\text{NLoS}}, & \text{if NLoS link,} \end{cases}$$
(1)

where μ_{LoS} and μ_{NLoS} are excessive attenuation factors for the LoS and the NLoS links, respectively, α is the path-loss exponent, $d_{i,j}, \forall i, j$ is the distance between nodes i and j, $K_o = \frac{4\pi f_c}{c}$ with c the speed of light, and f_c is the carrier frequency. As we assume LoS links between the UAVs, the path-loss model between UAV i and UAV j is given by [37]:

$$L_{i,j}^{\text{A2A}} = (K_o d_{i,j})^{\alpha} \mu_{\text{LoS}}.$$

For the A2G channel, the probability of having an LoS link is given by [37]–[39]:

$$P_{i,j}^{\text{LoS}} = \frac{1}{1 + \psi \exp(-\eta[\theta_{ij} - \psi])},$$
 (2)

where ψ and η are constants depending on the carrier frequency and the conditions of the environment. In (2), θ_{ij} denotes the elevation angle between node i and j given by:

$$\theta_{i,j} = \frac{180}{\pi} \times \sin^{-1} \left(\frac{\Delta z_{i,j}}{d_{i,j}} \right),$$

where $\Delta z_{i,j}$ is the difference in height between node i and node j. Consequently, the probability of NLoS link is given by $P_{i,j}^{\text{NLoS}} = 1 - P_{i,j}^{\text{LoS}}$. The average path-loss of the A2G link from node i to the node j is then obtained as:

$$\bar{L}_{i,j}^{\rm A2G} = (K_o d_{i,j})^{\alpha} [P_{i,j}^{\rm LoS} \times \mu_{\rm LoS} + P_{i,j}^{\rm NLoS} \times \mu_{\rm NLoS}].$$

Based on this, the channel power gain between a UAV i and a ground/aerial node j is given by:

$$h_{ij} = \begin{cases} \frac{1}{L_{i,j}^{A2A}}, & A2A \text{ link}, \\ \frac{1}{\bar{L}_{ij}^{A2G}}, & A2G \text{ link}. \end{cases}$$
(3)

We assume perfect channel reciprocity for all the links under consideration, i.e., $h_{ij} = h_{ji}$, $\forall i, j$. We also define the

$$\Gamma_{ij} = \begin{cases} (K_o^\alpha \mu_{\text{LoS}})^{-1}, & \text{A2A link,} \\ (K_o^\alpha [P_{i,j}^{\text{LoS}} \times \mu_{\text{LoS}} + P_{i,j}^{\text{NLoS}} \times \mu_{\text{NLoS}}])^{-1}, & \text{A2G link,} \end{cases}$$

which will be used later.

C. Graph Representation of the Network

We assume that the interference coming from the interferers is much stronger than the noise. We therefore take into account the signal-to-interference ratio (SIR) instead of signal-to-interference-plus-noise ratio (SINR), which is defined at node j for the transmitted signal from node i as follows:

$$SIR_{i,j} = \frac{P_i h_{i,j}}{\sum_{m \in \mathcal{M}} P_m^J h_{m,j}},$$
(4)

where P_i is the transmit power of UAV i, and P_m^J is the transmit power of interferer $m \in \mathcal{M}$ in the primary network. We further define $\mathbf{P} = [P_1, \dots, P_N]$ and $\mathbf{P}^J = [P_1^J, \dots, P_M^J]$.

We first define a flow graph $G = (\mathcal{N}, \mathcal{E})$, in which \mathcal{E} denotes the set of available edges in the network and each edge has the capacity $a_{i,j}, \forall i, j$. We assume a line topology for the multi-hop relay network as in [13] since the major data exchange happens between neighboring UAVs, not between the UAVs away by more than a single hop. Note that all the UAV relays are involved in data transmission from the BS to the UE. The "route" in our setting solely means the order in which the UAVs pass data from one to another, e.g., BS \rightarrow UAV 1 \rightarrow UAV 2 \rightarrow ... \rightarrow UAV $N \rightarrow$ UE, which we assumed to be known as in the literature concerning multi-hop UAV relaying [13], [14], [17], [18], [23]–[29]. We formulate the data communication in this single-source and single-destination network as a single-commodity maximum flow problem, for which the task is to maximize the flow between the BS and the desired UE. It is worth noting that our proposed framework is general enough to accommodate general network topology and other network flow problems. The average transmission rate is defined as the arithmetic mean of the data rates in the forward and backward directions for each pair of nodes. The generalized adjacency matrix is accordingly defined as $\mathbf{A} = [a_{i,j}]_{\{i,j\}=1}^N$, where $a_{i,j}$ is the average transmission rate between nodes i and j, given by:

$$a_{i,j} = \begin{cases} \frac{1}{2} B(\log_2(1 + \operatorname{SIR}_{i,j}) + \log_2(1 + \operatorname{SIR}_{j,i})), & i \neq j, \\ 0, & i = j, \end{cases}$$
(5)

with B the transmission bandwidth of the network. Note that $SIR_{i,j}$ is, in general, not equal to $SIR_{j,i}$, in part, due to the unbalanced deployment of interferer. We further define the *generalized degree matrix* of the network as $\mathbf{D} = \text{diag}\{\beta_1,\ldots,\beta_N\}$, where $\beta_i = \sum_{\{j|j\neq i\}} a_{i,j}$. Finally, the *Laplacian matrix* of the network graph is given by $\mathbf{L} = \mathbf{D} - \mathbf{A}$. In the following two sections, we formulate the 3D trajectory and power allocation problem under two different types of interferers. In particular, we consider *unintentional* and *intentional* (i.e., smart) interferers in sequence, and propose a solution for each case.

III. Unintentional Interferer

We first consider the unintentional interference for which the primary role of the interferer is not generating interference in our UAV-assisted network on purpose, but rather transmitting data to its desired UEs, as shown in Fig. 1. This type of interference is mainly caused by the transmitters within the existing network (e.g., neighbouring BSs, small cells), and hence is *unintentional*. This interferer can be static or mobile.

Since the UAVs are co-existing with the primary network, they must satisfy the interference constraint at primary receivers as well. We assume that the interferers (which can serve as BSs in primary network) are serving a set of primary UEs, which their quality of service (QoS) should be satisfied. Moreover, the transmission quality from primary UEs to the interferers in uplink should be maintained. We denote the set of all *primary UEs* in the primary network by \mathcal{U} , where their locations are given by $\mathbf{r}_u = (x_u, y_u, z_u) \in \mathbb{U}^3$ with $u \in \mathcal{U}$. The interferers and the UAV network can be either cooperative or non-cooperative. In the case of cooperation, the primary

transmitters can adjust their transmission powers to avoid generating excessive interference to the UAV network while satisfying their user's QoS. In real scenarios, the cooperation assumption might not be able to be satisfied properly; however, it can provide some insights on the upper bound of the performance of the UAV network. In the absence of cooperation, the interferers in the primary network do not adjust their transmission powers. The SIR at each primary UE $u \in \mathcal{U}$ for the transmitted signal from transmitter $m \in \mathcal{M}$ while UAV i transmits at the same time is given by

$$SIR_{m,u,i} = \frac{P_m^J h_{m,u}}{P_i h_{i,u} + \sum_{m' \in \mathcal{M}, m' \neq m} P_{m'}^J h_{m',u}},$$
 (6)

where the first term in the denominator is the interference from the UAV transmitting at the same time slot, and the second term is the interference from other primary BSs. Thus, the transmission rate between primary UE u and interferer m while the UAV i is transmitting at the same time is given by: $R_{m,u,i} = B \log_2(1 + \mathrm{SIR}_{m,u,i})$. In order to guarantee the QoS of the primary UEs, their transmission rates should be larger than a predefined threshold R^{th} .

A. Optimization Problem Formulation

We formulate the optimization problem, where the goal is to maximize the data flow f_s between the terrestrial BS and the desired UE with the help of relaying UAVs in the presence of interferers. The flow of the network can be assumed as a measure of average uplink/downlink transmission capability of the UAV network. For each link $(i,j) \in \mathcal{E}$, $f_{i,j}$ and $f_{j,i}$ are the amount of flows going from i to j and coming from j to i, respectively. The desired optimization problem for the cooperative case is therefore given as follows [40], [41]:

$$\max_{\substack{\mathbf{P}, \mathbf{P}^J, \{\mathbf{r}_i\}_{i \neq s, d}, \\ f_s, \ f_{i,j} \geq 0, \ \forall i,j}} f_s \tag{7}$$

s.t.
$$\sum_{j=1}^{N} (f_{i,j} - f_{j,i}) = f_s D_i, \quad \forall i \in \mathcal{N},$$
 (7a)

$$f_{i,j} + f_{j,i} \le a_{i,j}, \quad \forall i, j \in \mathcal{N},$$
 (7b)

$$d_{i,j} \ge d^{\text{safe}}, \quad \forall i, j \in \mathcal{N},$$
 (7c)

$$P_i h_{i,m} \le I_m^{\text{max}}, \quad \forall i \in \mathcal{N}, m \in \mathcal{M},$$
 (7d)

$$P_i < P_{\text{max}}, \quad \forall i \in \mathcal{N},$$
 (7e)

$$R_{m,u,i} \ge R^{\text{th}}, \quad \forall m \in \mathcal{M}, u \in \mathcal{U}, i \in \mathcal{N}, \quad (7f)$$

where D_i is equal to +1 for the source (i=s) to represent that the flow only goes out from the source, and it is equal to -1 for the destination (i=d) as the sink absorbs all the incoming flow. For the other nodes, the corresponding D_i 's are set to 0 to preserve balanced flows. The location of node $i \in \mathcal{N}$ in the UAV network is denoted by $\mathbf{r}_i = (x_i, y_i, z_i) \in \mathbb{R}^3$ such that $i \in \mathcal{N}$, $\mathbf{R} = [\mathbf{r}_1, \dots, \mathbf{r}_N]$, \mathbf{P}_{\max} is the maximum transmission power of each UAV, and I_m^{\max} represents the predefined interference threshold of the m-th interferer. In addition, constraint (7a) is due to the assumption of balanced flows for all the nodes except the source and the destination. Constraint (7b) ensures that the two-way flow

of each link is less than the maximum capacity. Constraint (7c) is considered to guarantee a safety separation between the UAVs and other nodes in the UAV network (i.e., the BS, the desired UE, or the other UAVs) in order to have a proper flight performance [42], where d^{safe} is the safe distance for the proper flight of UAVs. Moreover, constraint (7d) satisfies the condition that the interference generated by each UAV at any interferer m is always less than a predefined threshold I_m^{max} . Constraint (7e) is imposed to limit the transmission powers of the UAVs. Constraint (7f) is a QoS service consideration for the UEs in the primary network which guarantees the downlink QoS of the primary users. By imposing this condition and adjusting the transmission powers of the primary network transmitters (which are interferers from the UAV network perspective), the primary network avoids generating stronger interference on the UAV network beyond satisfying the QoS constraints. It is worth noting that with fixed locations for UAVs, solely optimizing the UAV transmission powers leads to a worse performance of the UAV relay network and vice versa. Thus, joint power allocation and 3D trajectory design is necessary to obtain the satisfactory performance for both networks. It is worth noting that in the case of non-cooperation, the optimization problem (7) is solved only with respect to the transmit power of the UAV **P** and their locations $\{r_i\}_{i\neq s,d}$, while the interferer's transmit power \mathbf{P}^{J} is determined by the primary network. Thus, the interferers may generate stronger interference which degrades the maximum flow of the UAV networks.

In the following, we to decompose the overall optimization of (7) into two sub-problems using the alternating-optimization approach [43]. In the proposed strategy, we first solve the 3D trajectory optimization for a given set of transmission powers (i.e., $P_i, \forall i \in \mathcal{N}$), and then the power allocation problem is solved for the given the locations of UAVs computed beforehand. These recursions continue till a satisfactory level of performance is obtained.

B. 3D Trajectory Optimization

We first attempt to solve the optimization problem in (7) to obtain the 3D trajectories of the UAVs assuming a given initial set of transmission powers. The optimization problem therefore reduces to a maximum flow problem with respect to the locations, which is given by:

$$\max_{ \substack{ \{\mathbf{r}_i\}_{i\neq s,d}, \\ f_s, \ f_{i,j} \geq 0, \ \forall i,j } } f_s$$
 s.t. (7a), (7b), (7c). (8)

Note that the maximum flow problem in (8) can be solved for given UAV transmission powers using the well-known max-flow-min-cut theorem [44]. Given the locations of the UAVs, the achievable maximum flow of the network is equal to the single flow min-cut of the underlying network given by:

$$f_{s} = \min_{\{S: v_{s} \in S, v_{d} \in \bar{S}\}} \sum_{i \in S, j \in \bar{S}} a_{i,j}, \tag{9}$$

where s denotes the source and d is the destination, and $S \subset \{1, \dots, N\}$ denotes a subset of nodes in the network

graph. The maximum flow in (9) can be obtained by the Ford-Fulkerson algorithm [44]. The challenging task is to design the trajectories (i.e., moving directions) of each UAV in the 3D space so as to maximize the information flow between the BS and the desired UE. The constraints (7a) and (7b) are implicitly satisfied by deploying the Ford-Fulkerson algorithm. Since the proposed solution for the trajectory design problem requires an unconstrained optimization, we further incorporate (7c) into the definition of the weights of the graphs. This is carried out via adding a penalty term to the edge capacity to define the *modified edge capacities* as follows:

$$\hat{a}_{i,j} = a_{i,j} - \chi \sum_{k \in \mathcal{N}} u(d_{j,k}/d_{\text{safe}}), \ \forall i, j,$$
 (10)

where χ stands for the importance of this safety precaution, and u(.) is the smoothed step function given by [45]:

$$u(y) = \zeta \frac{\exp(-\kappa y - \log y_0)}{1 + \exp(-\kappa y - \log y_0)},\tag{11}$$

where y_0 is an arbitrarily small positive number, and ζ and κ are design parameters. The parameter d^{safe} controls the minimum distance between any two nodes in the UAV networks to avoid collision. For instance, if the two UAVs i and j get too close to each other, the separation $d_{i,j}$ becomes much less than d^{safe} , which decreases the ratio $d_{i,j}/d^{\text{safe}}$ and forces the penalty $u(d_{i,j}/d^{\text{safe}})$ to increase dramatically. The modified edge capacity therefore decreases significantly, which is an undesired outcome in terms of our primary goal of maximizing the flow. As a result, our 3D trajectory design methodology will automatically avoid this unfavorable situation. Note that the parameters of the smoothed step function should be chosen properly so that the safety constraint is satisfied.

Although the proposed methods in the literature concerning UAV trajectory design are useful, they cannot be applied to our study for 3D trajectory design for a general setting with multi-hop relays and multiple interferers to optimize the maximum flow of a general graph. As can be seen in (4), the SIR expression is non-convex with respect to the locations of the UAVs [13], [14], which makes the maximum flow problem complicated to solve. In order to move the UAV to achieve the maximum flow of the network, we use *Cheeger constant* or *isoperimetric number* of the graph, which provides a numerical measure on how well-connected our UAV network is [46]. Assuming that $\mathcal{L} = \mathbf{D}^{-1/2}\mathbf{L}\mathbf{D}^{-1/2}$ is the normalized Laplacian matrix, the Cheeger constant is given as [46]

$$h(\mathcal{L}) = \min_{S} \frac{\sum_{i \in S, j \in \bar{S}} \hat{a}_{i,j}}{\min\{|S|, |\bar{S}|\}}, \tag{12}$$

where $S \subset \mathcal{N}$ is a subset of the nodes that contains the source but not the destination, $\bar{S} = \mathcal{N} - S$, and |S| is S cardinality. Note that the original definition of the Cheeger constant $h(\mathcal{L})$ considers all the nodes in the network with equal importance. Since the maximum flow of the network for a given source-destination pair depends on the individual link capacities, the weighted the Cheeger constant is a promising solution. In particular, the original Cheeger constant blindly aims at improving the weakest link in the network and may fail to emphasize the desired flow associated with a particular

source-destination pair. The weighted Cheeger constant is given as [45]:

$$h_{\mathbf{W}}(\mathcal{L}) = \min_{S} \frac{\sum_{i \in S, j \in \bar{S}} \hat{a}_{i,j}}{\min\{|S|_{\mathbf{W}}, |\bar{S}|_{\mathbf{W}}\}},$$
(13)

where $|S|_{\mathbf{W}} = \sum_{i \in S} w_i$ is the weighted cardinality, and $w_i \ge 0$ is the weight of node i. The weighted Laplacian matrix is then given by:

$$\mathcal{L}_{\mathbf{W}} = \mathbf{W}^{-1/2} \mathcal{L} \mathbf{W}^{-1/2}, \tag{14}$$

where $\mathbf{W} = \operatorname{diag}\{w_1, \dots, w_n\}$. Usually, the Cheeger constant is difficult to compute. To address this issue, the weighted algebraic connectivity $\lambda_2(\mathcal{L}_{\mathbf{W}})$ can be considered as a suitable alternative, which is given by:

$$\lambda_2(\mathcal{L}_{\mathbf{W}}) = \min_{\mathbf{v} \neq \mathbf{0}, \mathbf{v} \perp \mathbf{W}^{1/2} \mathbf{1}} \frac{\langle \mathcal{L}_{\mathbf{W}} \mathbf{v}, \mathbf{v} \rangle}{\langle \mathbf{v}, \mathbf{v} \rangle}.$$
 (15)

It is shown in [45] that the following weighted Cheeger's inequalities hold:

$$\lambda_2(\mathcal{L}_{\mathbf{W}})/2 \le h_{\mathbf{W}}(\mathcal{L}_{\mathbf{W}}) \le \sqrt{2\delta_{\max}\lambda_2(\mathcal{L}_{\mathbf{W}})/w_{\min}},$$
 (16)

where δ_{\max} is the maximum node degree, and $w_{\min} = \min_i w_i$. As can be seen, the larger values of $\lambda_2(\mathcal{L}_{\mathbf{W}})$ correspond to larger values of the lower bound of the weighted Cheeger constant. The UAVs can therefore adjust their geometric locations in order to maximize $\lambda_2(\mathcal{L}_{\mathbf{W}})$, and hence $h_{\mathbf{W}}(\mathcal{L})$.

We move each UAV along the *spatial* gradient of the weighted algebraic connectivity $\lambda_2(\mathcal{L}_{\mathbf{W}})$. Given the instantaneous location of the *i*th UAV, its spatial gradient along x-axis is given as follows:

$$\frac{\partial \lambda_2(\mathcal{L}_{\mathbf{W}})}{\partial x_i} = \mathbf{x}^{fT} \frac{\partial (\mathcal{L}_{\mathbf{W}})}{\partial x_i} \mathbf{x}^f = \sum_{p=1}^N \sum_{q=1}^N \frac{v_p^f}{\sqrt{w_p}} \frac{v_q^f}{\sqrt{w_q}} \left[\frac{\partial \mathcal{L}}{\partial x_i} \right]_{p,q}$$

$$= \sum_{\{p,q:p \sim q\}} \left[\frac{v_p^f}{\sqrt{w_p}} - \frac{v_q^f}{\sqrt{w_q}} \right]^2 \frac{\partial \hat{a}_{p,q}}{\partial x_i}, \tag{17}$$

where v_k^f is the kth entry of \mathbf{v}^f with $k \in \{p,q\}$, \mathbf{v}^f is the Fiedler vector which is the eigenvector corresponding to the second smallest eigenvalue $\lambda_2(\mathcal{L}_{\mathbf{W}})$, and $p \sim q$ means that the nodes p and q are connected. In (17), $\frac{\partial \hat{a}_{p,q}}{\partial x_i}$ can be computed as

$$\begin{split} \frac{\partial \hat{a}_{p,q}}{\partial x_{i}} &= \mathbf{B} \left[\frac{1}{1 + \mathrm{SIR}_{p,q}} \frac{\partial \mathrm{SIR}_{p,q}}{\partial x_{i}} + \frac{1}{1 + \mathrm{SIR}_{q,p}} \frac{\partial \mathrm{SIR}_{q,p}}{\partial x_{i}} \right] \\ &- \chi \sum_{k \in \mathcal{N}} u'(d_{q,k}/d^{\mathrm{safe}}) \frac{x_{k} - x_{q}}{d^{\mathrm{safe}}d_{q,k}}, \end{split} \tag{18}$$

which is 0 for p=q, or $i \notin \{p,q\}$. The Fiedler vector can be computed in a distributed manner as well [47]. The partial derivative of SIR with respect to x_i in (18) can be computed using (4) together with the geometrical relations between x_i and the channel gain $h_{i,j}$ presented in Section II-B. After obtaining the gradient $[\frac{\partial \lambda_2(\mathcal{L}\mathbf{w})}{\partial x_i(t)}, \frac{\partial \lambda_2(\mathcal{L}\mathbf{w})}{\partial y_i(t)}, \frac{\partial \lambda_2(\mathcal{L}\mathbf{w})}{\partial z_i(t)}]^T$ at the current time slot t, the UAVs move along the directions x and y respectively by distances:

$$dx(t) = v_m \cdot \cos(\theta) \sin(\phi) dt, \tag{19}$$

$$dy(t) = v_m \cdot \sin(\theta) \sin(\phi) dt, \tag{20}$$

$$dz(t) = v_m \cos(\phi) dt, \tag{21}$$

Algorithm 1 DC-Based SCA Algorithm for Power Allocation

- 1: **Initialization:** Iteration number $\ell := 1$, locations \mathbf{r}_i , $\forall i \in \mathcal{N}$, feasible initial value for $P_i[0]$, $\forall i \in \mathcal{N}$ and $\mathbf{P}^J[0]$.
- 2: Calculate the value of $\tilde{a}_{i,j}(P_i[0], P_j[0], \mathbf{P}^J[0]), \ \forall i \in \mathcal{N}$ using (31).
- 3: **while** $|\eta[\ell] \eta[\ell-1]| > \varepsilon$ **do**
- 4: Compute the optimal power allocation $P_i[\ell]$, $\forall i \in \mathcal{N}$ and $\mathbf{P}^J[\ell]$ in (36) using CVX [48].
- 5: Compute $\tilde{a}_{i,j}(P_i[\ell], P_j[\ell], \mathbf{P}^J[\ell]), \forall i \in \mathcal{N}$ using (31).
- 6: $\ell \leftarrow \ell + 1$
- 7: end while

where v_m is the moving speed of the UAV; $\theta = \arctan\left(\frac{\partial \lambda_2(\mathcal{L}_{\mathbf{W}})}{\partial y_i(t)}/\frac{\partial \lambda_2(\mathcal{L}_{\mathbf{W}})}{\partial x_i(t)}\right)$; $\phi = \arctan\left(\frac{\partial \lambda_2(\mathcal{L}_{\mathbf{W}})}{\partial z_i(t)}\right)$; dt is the length of the time slot. The update in the location of the ith UAV is then given as

$$x_i(t) = x_i(t-1) + dx(t),$$
 (22)

$$y_i(t) = y_i(t-1) + dy(t),$$
 (23)

$$z_i(t) = z_i(t-1) + dz(t),$$
 (24)

where t stands for the discrete time, or, equivalently, the iteration number.

C. Power Allocation Optimization

We now focus on the power allocation problem, and solve the optimization problem in (7) to find the optimal power allocation for a given set of the UAV locations. In this case, we consider the unintentional interferer generating the unwanted interference. We assume that the primary network and the UAV network can cooperate to mitigate the mutual interference. The UAVs try to mitigate the unwanted interference between the primary network and the UAV network to improve the data flow between the source and the destination. The corresponding optimization is given by:

$$\max_{\mathbf{P}, \mathbf{P}^{J}, f_{s}} f_{s}$$
s.t. (7a), (7b), (7c), (7d), (7e), (7f). (25)

In this case, the maximum data exchange of the network is determined by the link with the minimum edge capacity. Hence, as we try to maximize the flow of the network, we equivalently maximize the data exchange of the hop with the minimum instantaneous rate. More specifically, the power allocation problem can be equivalently given by

$$\max_{\mathbf{P}, \mathbf{P}^{J}} \min_{\forall i, j} a_{i, j}
\text{s.t. } (7d), (7e), (7f).$$
(26)

In order to have a more tractable problem, (26) can be reformulated as follows:

$$\max_{\mathbf{P}, \mathbf{P}^J, \eta} \eta \tag{27}$$

s.t.
$$0 \le \eta \le a_{i,j}, \forall i, j,$$

(7d), (7e), (7f), (27a)

where η is an auxiliary variable employed to facilitate the optimization. In this case, the objective is an affine function. However, the constraint on $a_{i,j}$ is not convex. $a_{i,j}$, $\forall i, j$, can be recast as the difference of two concave functions, given by $a_{i,j}(P_i, P_j, \mathbf{P}^J) = v(P_i, P_j, \mathbf{P}^J) - r_{i,j}(\mathbf{P}^J)$, where

$$v(P_{i}, P_{j}, \mathbf{P}^{J}) = \frac{1}{2} B \left[\log_{2} \left(P_{i} h_{i,j} + \sum_{m' \in \mathcal{M}} P_{m'}^{J} h_{m',j} \right) + \log_{2} \left(P_{j} h_{j,i} + \sum_{m' \in \mathcal{M}} P_{m'}^{J} h_{m',i} \right) \right], \quad (28)$$

and

$$r_{i,j}(\mathbf{P}^{J}) = \frac{1}{2} B \left[\log_2 \left(\sum_{m' \in \mathcal{M}} P_{m'}^{J} h_{m',j} \right) + \log_2 \left(\sum_{m' \in \mathcal{M}} P_{m'}^{J} h_{m',i} \right) \right].$$

$$(29)$$

In general, the difference of two concave functions is not a concave one [49]. In order to convexify this function at iteration ℓ , we deploy first-order Taylor expansion to approximate $r_{i,j}(\mathbf{P}^J)$ around a given point from the previous iteration $\mathbf{P}^J[\ell-1]$ as:

$$\tilde{r}_{i,j}(\mathbf{P}^J) \approx r_{i,j}(\mathbf{P}^J[\ell-1]) + (\nabla r_{i,j}(\mathbf{P}^J[\ell-1]))^T(\mathbf{P}^J - \mathbf{P}^J[\ell-1]).$$
(30)

Thus, we have the approximation of $a_{i,j}(P_i, P_j, \mathbf{P}^J)$ as:

$$\tilde{a}_{i,j}(P_i, P_j, \mathbf{P}^J) = v(P_i, P_j, \mathbf{P}^J) - \tilde{r}_{i,j}(\mathbf{P}^J). \tag{31}$$

Using this approximation, it can be verified that $\tilde{a}_{i,j}(P_i,P_j,\mathbf{P}^J)$ is a concave function. A similar approximation can be adopted for the constraint (7f) to make it a convex constraint as $(\hat{7}f)$. To do this, we can re-write the rate function in constraint (7f) as:

$$R_{m,u,i}(P_i, \mathbf{P}^J) = B\left(\log_2\left(P_i h_{i,u} + \sum_{m' \in \mathcal{M}} P_j^J h_{j,u}\right) - \log_2\left(P_i h_{i,u} + \sum_{m' \in \mathcal{M}, m' \neq m} P_j^J h_{m',u}\right)\right). \tag{32}$$

As can be seen in (32), $R_{m,u,i}(P_i, \mathbf{P}^J)$ is the difference of two concave functions. Since $R_{m,u,i}(P_i, \mathbf{P}^J)$ is on the right hand side of the inequality in constraint (7f), it should be a concave function to have a convex optimization problem [50]. However, the difference of two concave functions is not necessarily concave. Hence, we deploy the first order Taylor expansion to approximate the second concave function in (32), which results in $\hat{R}_{m,u,i}(P_i, \mathbf{P}^J)$ given by:

$$\hat{R}_{m,u,i}(P_i, \mathbf{P}^J) = B\left(\log_2\left(P_i h_{i,u} + \sum_{m' \in \mathcal{M}} P_{m'}^J h_{m',u}\right) - \tilde{g}_{m,u,i}(\mathbf{p}_i)\right),$$

$$\tilde{g}_{m,u,i}(\mathbf{p}_i) = g_{m,u,i}(\mathbf{p}_i[\ell-1]) + (\nabla g_{m,u,i}(\mathbf{p}_i[\ell-1]))^T (\mathbf{p}_i - \mathbf{p}_i[\ell-1]),$$
(34)

where
$$g_{m,u,i}(\mathbf{p}) \approx \log_2 \Big(P_i \, h_{i,u} + \sum_{m' \in \mathcal{M}, m' \neq m} P_{m'}^J \, h_{m',u} \Big).$$

For notation simplicity, we consider $\mathbf{p}_i = [P_i, \mathbf{P}^J]$. Let $\mathbf{p}_i[\ell-1]$ denote the starting point of Taylor expansion obtained from previous iteration. Deploying Taylor expansion in each iteration, the approximated constraint is written as:

$$(\hat{7}f): R^{th} \leq \hat{R}_{m,u,i}(P_i, \mathbf{P}^J), \quad \forall m \in \mathcal{M}, u \in \mathcal{R}, i \in \mathcal{N}.$$
 (35)

Thus, the optimization problem in (27) can be recast as:

$$\max_{\mathbf{P}, \mathbf{P}^{J}, \eta} \eta$$
s.t. $0 \le \eta \le \tilde{a}_{i,j}, \forall i, j,$

$$(7d), (7e), (7f).$$
(36a)

After substituting the approximated versions of the constraints, in each iteration ℓ , the above optimization problem is now convex, which can be solved efficiently using the interior point method [50]. This procedure, called successive convex approximation (SCA) [51], is described in Algorithm 1, which generates a sequence of improved feasible points that converge to at least a local optimal point $(\mathbf{P}^*, \mathbf{P}^{J*})$ [52]. If the primary network does not cooperate with the UAV network, the optimization can be written with respect to the UAVs' transmit powers while the transmit powers of the existing network are fixed.

D. The Alternating Optimization Algorithm

- 1) Algorithm Description: Given the transmission powers of the UAVs, the trajectory design problem can be solved based on the Cheeger constant in Section III-B. Given the locations of the UAVs, the power allocation can be obtained using the SCA method as in Algorithm 1 discussed in Section III-C. At each step of 3D trajectory design, we need to make sure that the interference threshold constraint is met in the primary network. Thus, at each iteration of the 3D trajectory design, we compute new set of transmit powers for UAVs. The overall algorithm considering both the 3D trajectory and power allocation optimization is summarized in Algorithm 2.
- 2) Convergence Analysis: In this part, we analyze the convergence of each sub-problem considered in Algorithm 2. The power allocation optimization (Algorithm 1) is in the format of difference of concave functions, which is not necessarily concave. Thus, the global optimal solution can be obtained only using exhaustive search. Nonetheless, based on our developed DC programming method in Algorithm 1, we can assure that our proposed power allocation solution converges to a local optimal point.

Proposition 1: Algorithm 1 is guaranteed to provide a monotonically increasing sequence of improved solutions over the iterations $\{\eta_\ell\}_{\ell\geq 0}$ which converge to a local optimal point of the problem (36).

Proof: At each iteration ℓ , the proposed SCA method approximates the non-convex functions in the optimization problem using the first order Taylor expansion. As in (30), since $r_{i,j}(\mathbf{P}^J)$ is a concave function, its gradient is also its

Algorithm 2 Proposed Alternating-Optimization Algorithm

Initialization: Locations \mathbf{r}_i and power allocation P_i for ith UAV for $\forall i \in \mathcal{N} \cup \mathcal{M}$, error tolerance ε $t \leftarrow 1$, $f_{\mathrm{s}}(-1) \leftarrow -\infty$, $f_{\mathrm{s}}(0) \leftarrow 0$ while $|f_{\mathrm{s}}(t-1) - f_{\mathrm{s}}(t-2)| > \varepsilon$ do

Compute $\frac{\partial \lambda_2(\mathcal{L}_{\mathbf{W}})}{\partial x_i(t)}$, $\frac{\partial \lambda_2(\mathcal{L}_{\mathbf{W}})}{\partial y_i(t)}$, $\frac{\partial \lambda_2(\mathcal{L}_{\mathbf{W}})}{\partial z_i(t)}$ by (17). Update $\mathbf{r}_i(t)$ in \mathbb{R}^3 as in (22), (23), (24). Compute optimal \mathbf{P} and \mathbf{P}^J using SCA algorithm given in Algorithm 1. Compute $f_{\mathrm{s}}(t)$ by Ford-Fulkerson algorithm [44] $t \leftarrow t+1$ end while

super-gradient [53], and thus we have:

$$r_{i,j}(\mathbf{P}^{J}) \leq r_{i,j}(\mathbf{P}^{J}[\ell-1]) + \langle \nabla r_{i,j}(\mathbf{P}^{J}[\ell-1]), \mathbf{P}^{J} - \mathbf{P}^{J}[\ell-1] \rangle.$$
(37)

This provides a proper approximation that makes (36) a lower bound maximization problem for the non-convex problem given in (27). Therefore, the proposed method provides a sequence of improved solutions over the iterations. Moreover, the constraint set of the optimization problem (36) is compact. As a result, according to Cauchy theorem [53], the sequence $\{\eta_\ell\}_{\ell\geq 0}$ always converges to a local optimal point.

As to the trajectory design sub-problem, we maximize the upper bound of the Cheeger constant which is the algebraic connectivity of the network graph. Since we deploy the gradient descent method for the optimization [54], it converges to a local optimum of the second smallest eigenvalue. In the simulation results, we empirically demonstrate that our proposed algorithm continuously moves toward increasing the network flow of the network until convergence.

3) Computational Complexity: We analyze the computational complexity of the proposed alternating optimization solution for the problem in (7). Algorithm 2 includes two sub-problems based on the DC programming and Cheeger constant optimization approaches, the complexity of each of which is discussed below.

Regarding the DC programming approach described in Algorithm 1, since (36) is a convex problem, we deploy the CVX optimization toolbox [55] with interior point method [50] at each iteration ℓ . The interior point method requires $\log(N_c/t^0\rho)/\log(\zeta)$ number of iterations (Newton steps) to solve a convex optimization problem, where $N_c = N^2 +$ NM + N + NMU is the total number of constraints in (36), $t^0 > 0$ is the initial point for approximating the indicator function in the barrier method, $0 < \rho \ll 1$ is the stopping criterion and $\zeta > 1$ is used to update the accuracy of the interior point [56]–[58]. According to [50], the values of 10 to 20 work well for ζ and a proper value for t^0 can be 2. Regarding the trajectory design sub-problem, the computational complexity is dominated by the computation of the Fiedler vector required in (17). The Fielder vector can be obtained with a worst-case computational complexity of $O(N^3)$ [59]. The overall complexity of the Algorithm 2 is

given by $\mathcal{O}\left(N_T\left(N_P\frac{\log(N_c/t^0\rho)}{\log(\zeta)}+N^3\right)\right)$, where N_P and N_T are the number of required iterations for convergence of Algorithm 1 and 2, respectively.

Alternatively, the Fiedler vector can be computed in a distribute manner at the UAVs, where each UAV computes its associated element of the Fiedler vector. This can be achieved efficiently via the method proposed in [47], with a worst-case computational complexity of $c+2|\mathcal{N}_k|$ floating point operations (flops) per iteration at each UAV, where \mathcal{N}_k denotes the set of neighboring nodes of UAV k and c is some constant. This distributed method is guaranteed to converge to the Fiedler vector, and requires each UAV to transmit two scalars to each of its neighbors during each iteration of the algorithm, which does not impose significant communication burden.

IV. SMART INTERFERER

In this section, we assume that smart interferers can purposefully move in order to decrease the flow of the UAV network (see Fig. 2). The moving smart interferers can be assumed as other UAVs trying to interrupt or degrade the quality of the communication quality of the legitimate UAVs. In this case, the UAVs act selfishly to improve their own transmission quality. This implies that the interference on the co-existing network, i.e., the smart jammer UAVs, is redundant and can be dropped. We consider the problem from both the UAV network and the smart interferer's perspectives. The UAVs in the UAV network try to reconfigure their 3D locations to evade the interference caused by the smart interferers, while the smart interferers' goal is to chase the UAVs to decrease the path-loss effect and hence increase the intended interference to the UAV network. In this case, the UAVs can transmit with their maximum powers. Hence, the optimization problem only comprises the trajectory design given by:

$$\max_{f_{s}, f_{i,j} \geq 0, \ \forall i,j, \ \{\mathbf{r}_{i}\}_{i \neq s,d}} f_{s}$$
s.t.
$$\sum_{j=1}^{N} (f_{i,j} - f_{j,i}) = f_{s} D_{i}, \ \forall i \in \mathcal{N},$$
 (38a)
$$f_{i,j} + f_{j,i} \leq a_{i,j}, \ \forall i, j \in \mathcal{N}.$$
 (38b)

In the following, we address the problem from the perspectives of both the UAV network and the smart jammers.

A. From the UAV Network Perspective

In the UAV network, the UAVs try to evade the smart interferers' interference. For the power allocation, since there are no constraints on the interference of the UAVs to smart jammers, the best strategy is to transmit with full power. In the 3D trajectory design, the UAVs move toward the spatial gradients of the algebraic connectivity to maximize the flow of the network as in (17).

B. From the Smart Interferers' Perspective

Here, we consider the problem from the perspective of moving smart interferers which can be assumed as other UAVs aiming at decreasing the flow of the network. To this end,

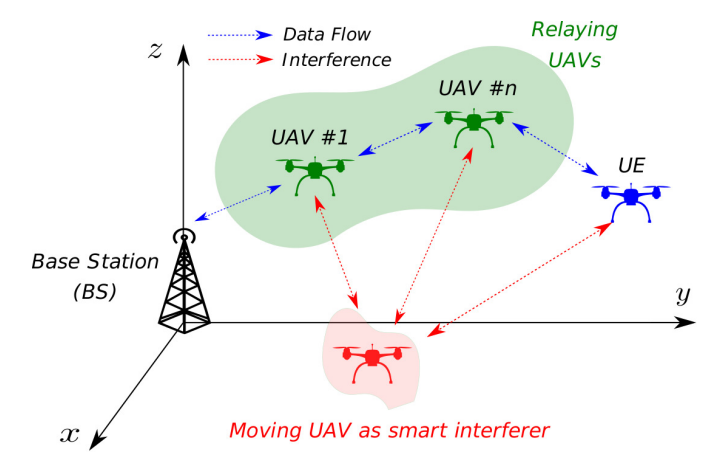


Fig. 2. System model for the communications scenario where the interferer is a smart moving UAV.

we assume that the smart UAVs transmit with their full power and move towards the opposite direction of the spatial gradient of the algebraic connectivity of the UAV network weighted Laplacian matrix. Thus, the moving direction for the moving smart interferers is given by:

$$\frac{\partial \lambda_{2}(\mathcal{L}_{\mathbf{W}})}{\partial x_{m}^{J}} = -\mathbf{x}^{f} \frac{\partial (\mathcal{L}_{\mathbf{W}})}{\partial x_{m}^{J}} \mathbf{x}^{f} = -\sum_{p=1}^{N} \sum_{q=1}^{N} \frac{v_{p}^{f} v_{q}^{f}}{\sqrt{w_{p} w_{q}}} \left[\frac{\partial \mathcal{L}}{\partial x_{m}^{J}} \right]_{p,q}$$

$$= -\sum_{\{p,q:p \sim q\}} \left[\frac{v_{p}^{f}}{\sqrt{w_{p}}} - \frac{v_{q}^{f}}{\sqrt{w_{q}}} \right]^{2} \frac{\partial a_{p,q}}{\partial x_{m}^{J}}, \quad \forall m \in \mathcal{M}.$$

$$(40)$$

By moving along the opposite direction of spatial gradient of the second smallest eigenvalue of the weighted Laplacian matrix of the UAV network, the smart interferers can decrease the maximum flow between the BS and the UE. The partial derivative of the SIR between two node i and j with respect to $x_m^J, \ \forall \ m \in \mathcal{M},$ can be obtained similar to (18). We consider a parameter τ so as to adjust the level of smartness of the smart UAV. That means the smart UAV interferer can move every τ iterations. Thus, by decreasing the value of τ the moving interferer will be smarter as it can chase the relay UAVs faster. It should be noted that we consider the static interferer as naive interferer in this scenario.

V. SERVING MULTIPLE UES: A MULTI-COMMODITY FLOW APPROACH

Although the models considered in Section III and Section IV are common in the literature as shown in Table I, where the UAVs are utilized to serve only one UE, we take one step further and extend our work to the multiple UE setting. In this case, we formulate the problem as a multi-commodity flow problem in which each UAV may be deployed in the paths of data flows from multiple BSs to multiple UEs. We mainly investigate the 3D trajectory design in this scenario. Due to the fact that UAVs may serve in data relaying for multiple UEs, the power allocation problem for the case of unintentional interferers is highly non-trivial and obtaining the optimal solution is very challenging. Thus, we will resort to a heuristic

method to tackle the power allocation. For the case of smart interferers, all the nodes transmit with full power in both sides in the arms race.

A. 3D Trajectory Design

We consider a scenario where multiple BSs in set \mathcal{B} serve K UEs in set \mathcal{K} . Let N denote the number of BSs, UEs, and UAVs in the network. We extend our single commodity flow formulation to the multi-commodity flow problem in this setting [41], [60]. In our formulation, we assume K commodities (data flows) each having its own source $v_{s_k} \in \mathcal{B}$, destination $v_{d_k} \in \mathcal{K}$, and demand $D^{(k)}$ for $1 \leq k \leq K$. It is worth noting that the sources or destinations can be the same for some flows. We define the maximum concurrent flow as the maximum f_m so that $f_m D^{(k)}$ units of data flow k, $1 \leq k \leq K$, can be transmitted simultaneously without exceeding the edge capacity. More specifically, the multicommodity flow problem can be written as follows:

$$\max_{f_m, \ f_{i,j}^{(k)}, \ \forall \ i,j,k, \ \{\mathbf{r}_i\}_{i\neq s,d}} f_m \tag{41}$$

s.t.
$$\sum_{j=1}^{N} \left(f_{i,j}^{(k)} - f_{j,i}^{(k)} \right) = f_m D_i^{(k)}, \quad \forall i, k \quad (41a)$$

$$\sum_{k=1}^{K} \left(f_{i,j}^{(k)} + f_{j,i}^{(k)} \right) \le a_{i,j}, \quad \forall i, j$$
 (41b)

$$f_{i,j}^{(k)} \ge 0, \quad \forall i, j, k \tag{41c}$$

where $f_{i,j}^{(k)}$ and $f_{j,i}^{(k)}$ are the amount of data flow k from node i to node j and that from node j to node i, respectively. $D_i^{(k)}$ is introduced to keep flows balanced, which is equal to $+D^{(k)}$ or $-D^{(k)}$ if node i is the source or the destination for data flow k, respectively, and 0 in all other cases. A typical choice for the equally important commodities is $D^{(k)} = 1/K$. The maximum flow of the multi-commodity problem can be obtained using the minimum multicut C_m as in [60]:

$$C_m = \min_{S} \frac{\sum_{i \in S, j \in \bar{S}} a_{i,j}}{\sum_{k \in \mathcal{K}(S)} D^{(k)}},\tag{42}$$

where $\mathcal{K}(S)=\{k: v_{s_k}\in S \text{ and } v_{d_k}\in \bar{S}, \text{ or } v_{s_k}\in \bar{S} \text{ and } v_{d_k}\in \bar{S}\}.$ Similar to the single commodity case, the UAVs can max-

Similar to the single commodity case, the UAVs can maximize $\lambda_2\left(\mathcal{L}_{\bar{\mathbf{W}}}^{(K)}\right)$ to design their trajectories, where $\bar{\mathbf{W}}=\mathrm{diag}\{\bar{w}_1,\ldots,\bar{w}_N\},\ \bar{w}_i=\sum_{k=1}^K(w_i^{(k)})^{1-p}$ with $w_i^{(k)}$ the weight assignment for flow k at node i, and $p\in[0,1)$ a design parameter. The weighted Laplacian matrix is given by $\mathcal{L}_{\bar{\mathbf{W}}}^{(K)}=\bar{\mathbf{W}}^{-1/2}\mathcal{L}\bar{\mathbf{W}}^{-1/2}$ [45]. It is worth noting that the above formulations is general enough to cover both the multi-cast and multi-uni-cast scenarios. In the multi-cast scenario, there exists one BS (source) and multiple UEs (destinations), while in the multi-uni-cast scenario, there are multiple BS (source) and UE (destination) pairs each transmitting their own data.

B. Power Allocation for Unintentional Interferers

For the power allocation, we consider deploying the same transmit powers at the UAVs $P_i = P_u, \forall i \in \mathcal{N}$. To obtain

TABLE II
SIMULATION PARAMETERS

Parameter	Value
Path-loss exponent α	2
Maximum transmit power of the UAVs (P_{max})	$20\mathrm{dBm}$
Transmit power of the interferers $(P_m^J, \forall m \in \mathcal{M})$	$30\mathrm{dBm}$
Bandwidth (B)	10 KHz
Interference threshold $(I_m^{\text{th}}, \forall m \in \mathcal{M})$	[-50, -10] dBm
Safety distance (d^{safe})	5 m
Carrier frequency (f_c)	2 GHz
Smoothed step-function parameters (ζ, κ, y_0)	$1, 10, 10^{-3}$
Penalty term coefficient (χ)	10^{4}
Additional path loss to free space for LoS (μ_{LoS})	3dB
Additional path loss to free space for NLoS (μ_{NLoS})	23 dB

 P_u in each iteration t of trajectory adaptation, we find the maximum power that satisfies the feasibility constraints (7d), (7f) concerning the interference limit and QoS requirement on the primary network. To this end, we deploy binary search in the interval $P_u \in [0, P_{\text{max}}]$ with quantization step β , and successively check those feasibility conditions until convergence, which is always achieved with time complexity of $\mathcal{O}(\log_2([P_{\text{max}}/\beta]))$. The more general power allocation problem will be left as a future work.

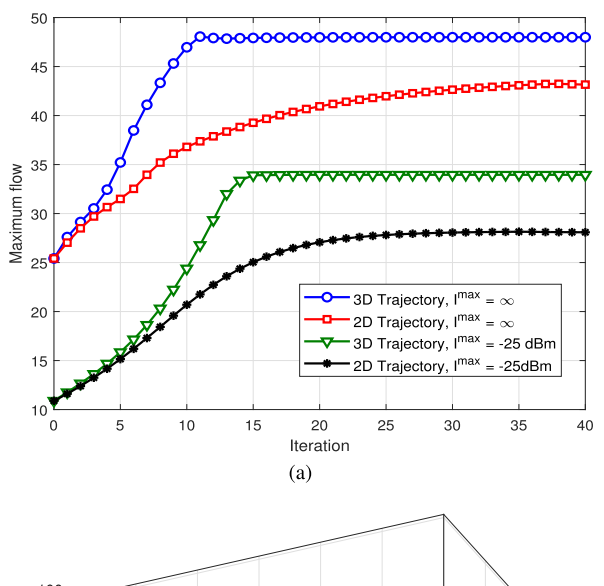
VI. SIMULATION RESULTS

In this section, we present numerical results to evaluate the performance of the proposed joint 3D trajectory and power allocation optimization. In our simulation environment, the BS and the UE are assumed to be located at $(0,0,h^{\rm BS})$ and $(200,0,h^{\rm UE})$, respectively, in \mathbb{R}^3 with $h^{\rm BS}=15\,\mathrm{m}$ and the unintentional interferers are located randomly in xy- plane with fixed altitude of $h^{\rm Int}=15\,\mathrm{m}$ and $I^{\rm max}=-25\mathrm{dBm}$, unless otherwise stated. The list of simulation parameters are given in Table II. In the figures for trajectories of the UAVs, the black dots indicate the final locations of the UAVs. We choose the maximum speed of $v_m=5\,\mathrm{m/s}$ for the UAVs. We assume the communications occurs in an urban environment with $\psi=11.95$ and $\eta=0.14$ at 2GHz carrier frequency. We consider 10 primary UEs with QoS requirement of 1 bits/s/Hz.

In practice, the perfect estimation of the locations of the UAVs may not be feasible on both UAV network side and interferer's side. Thus, it is also important to examine how our proposed method performs in the presence of the localization errors. Here, we define δ as the localization error from the perfect location of the nodes as

$$\delta \triangleq \left| 1 - \left(\frac{\hat{d}_{i,j}}{d_{i,j}} \right) \right| \times 100,$$

where $\hat{d}_{i,j}$ and $d_{i,j}$ are the estimated and true distances for two given nodes i and j, respectively. In order to obtain samples $\hat{\mathbf{r}}_j$ with δ percent localization error around point \mathbf{r}_j , we generate uniform samples on a sphere with the center of \mathbf{r}_j and radius of $d_{i,j} \times \delta/100$. It is worth noting that our proposed approach only requires the distance between the nodes and the pathloss information. In all the simulations related to localization error, the results are averaged over 1000 Monte Carlo runs.



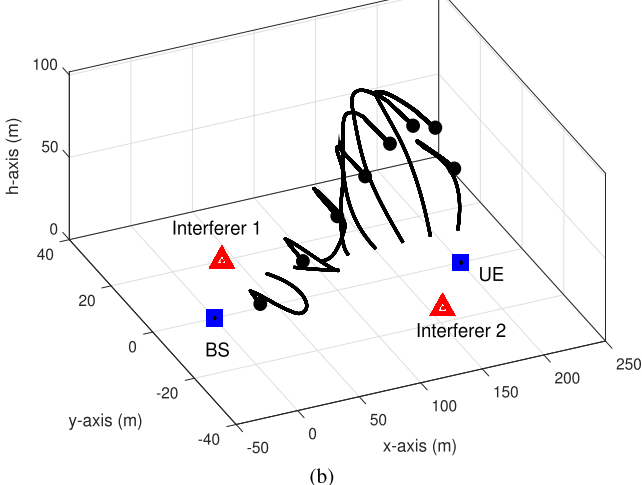


Fig. 3. Performance of the proposed approach for a single UE with 8 UAVs and 2 interferers (a) Convergence of the proposed alternating optimization problem. (b) 3D trajectories of the UAVs when $I^{\rm max} = -25$ dBm (3D view).

A. Unintentional Interferer

1) Convergence of the Proposed Algorithm: In Fig. 3a, the maximum flow of the network is depicted versus iterations, assuming 8 UAVs, 2 interferers, and a UE on the ground. Each iteration is composed of solving one power allocation optimization problem and one trajectory design. The results for different values of I^{\max} , which determines the maximum value of tolerable interference from the UAV network on the primary network. As can be seen, the larger the I^{\max} , the larger data flow can be achieved between the BS and the UE since the UAVs can transmit with more powers. In this figure, we show the maximum flow of the network for 2D and 3D trajectory design approaches. For the xy-plane 2D trajectory design, we assume that each UAV can move in xy-plane and it cannot move in z direction (its height is assumed to be fixed at 20 m). It can be seen that both algorithms converge in finite number of iterations. However, 3D trajectory design significantly outperforms the 2D trajectory design and can improves the maximum flow of the network considerably. This performance improvement is due to the fact that 3D space has more degrees of freedom as compared to 2D space. All

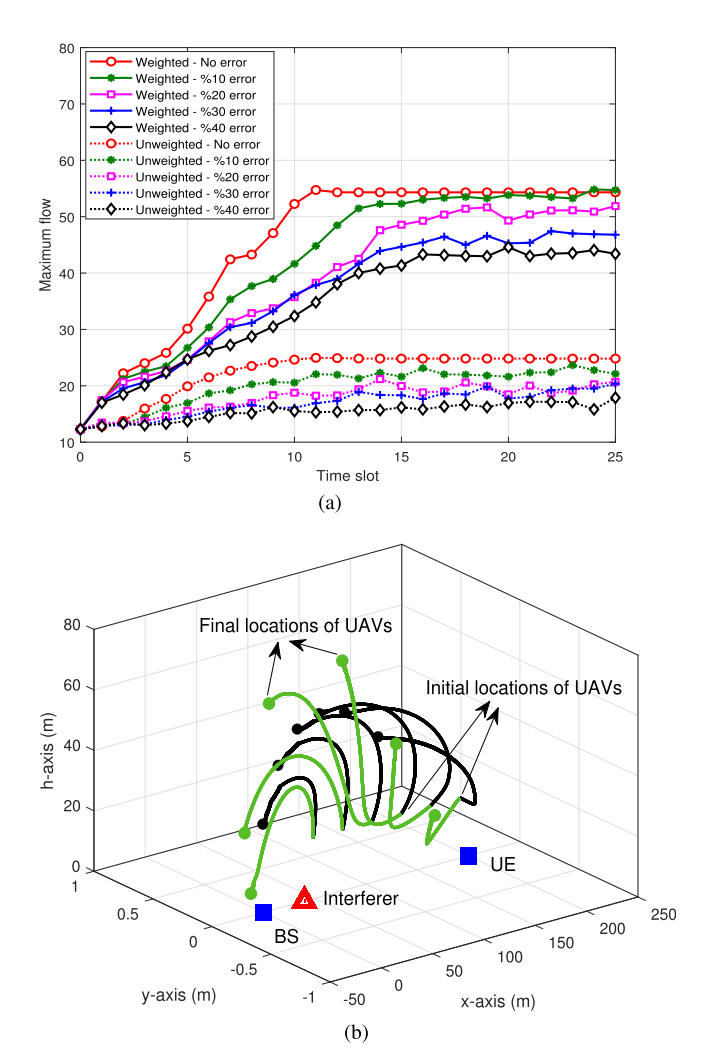


Fig. 4. (a) The maximum flow of the network for weighted and unweighted Cheeger constant for different localization errors. (b) Different trajectories for weighted and unweighted Cheeger constant when localization is perfect. Green and black trajectories are based on weighted and regular Cheeger constants, respectively.

the results presented in Fig. 3a are obtained using weighted Cheeger constant. In Fig. 3b, the 3D trajectories of the UAVs are shown. We observe that the relaying UAVs adjust their locations in 3D space so as to evade from the interferers, and therefore improve the desired data flow between the BS and the UE.²

2) Impact of Weighted Cheeger Constant: Here, we investigate the impact of using weighted version of Cheeger constant on the desired data flow and 3D trajectories. In Fig. 4a, we depict the maximum flow for the conventional Cheeger constant and weighted Cheeger constant with assuming 6 UAVs and one interferer. We consider different localization error values for the locations of the UAVs. We observe that the weighted version is significantly superior to the conventional one. As shown, even with localization error, the proposed approach can improve the maximum flow of the network. We also depict the corresponding 3D UAV trajectories

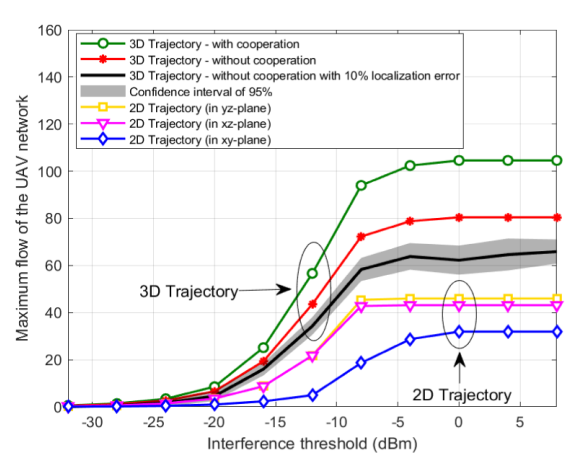


Fig. 5. Maximum flow versus interference threshold for 2D and 3D trajectory optimization strategies along with optimal power allocation.

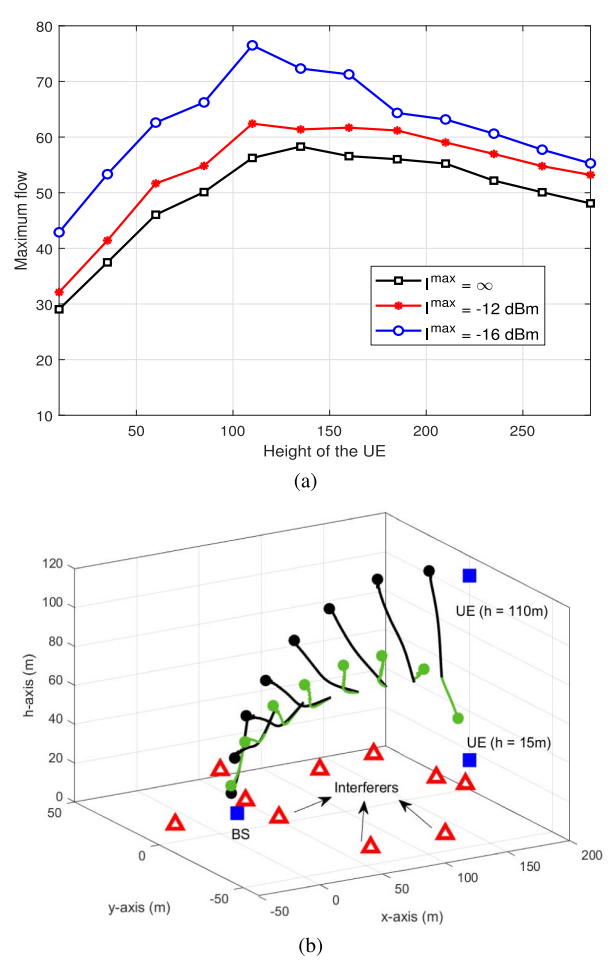


Fig. 6. (a) The maximum flow of the network with respect to height of the UE. (b) The 3D trajectories for UAVs, where green trajectories are for $h^{\rm UE}=15{\rm m}$ and black trajectories are for optimal UE height $h^{\rm UE}=110{\rm m}$.

in Fig. 4b. Interestingly, weighted Cheeger constant results in 3D trajectories ending up with final UAV locations closer to both the BS and UE. This might be due to the fact that the bottleneck of the network flow occurs at the closer links to the BS and the UE, considering the close proximity of the interferer located on the ground. The weighted Cheeger constant therefore adjusts the final UAV locations to make them as close to the BS and UE as possible.

²We assume that the UAVs are able to move freely to any locations in the air as long as they consider the safety distance from each other. In practice, there may be further constraints on the initial or final locations of the UAVs, which can be incorporated in our framework as well.

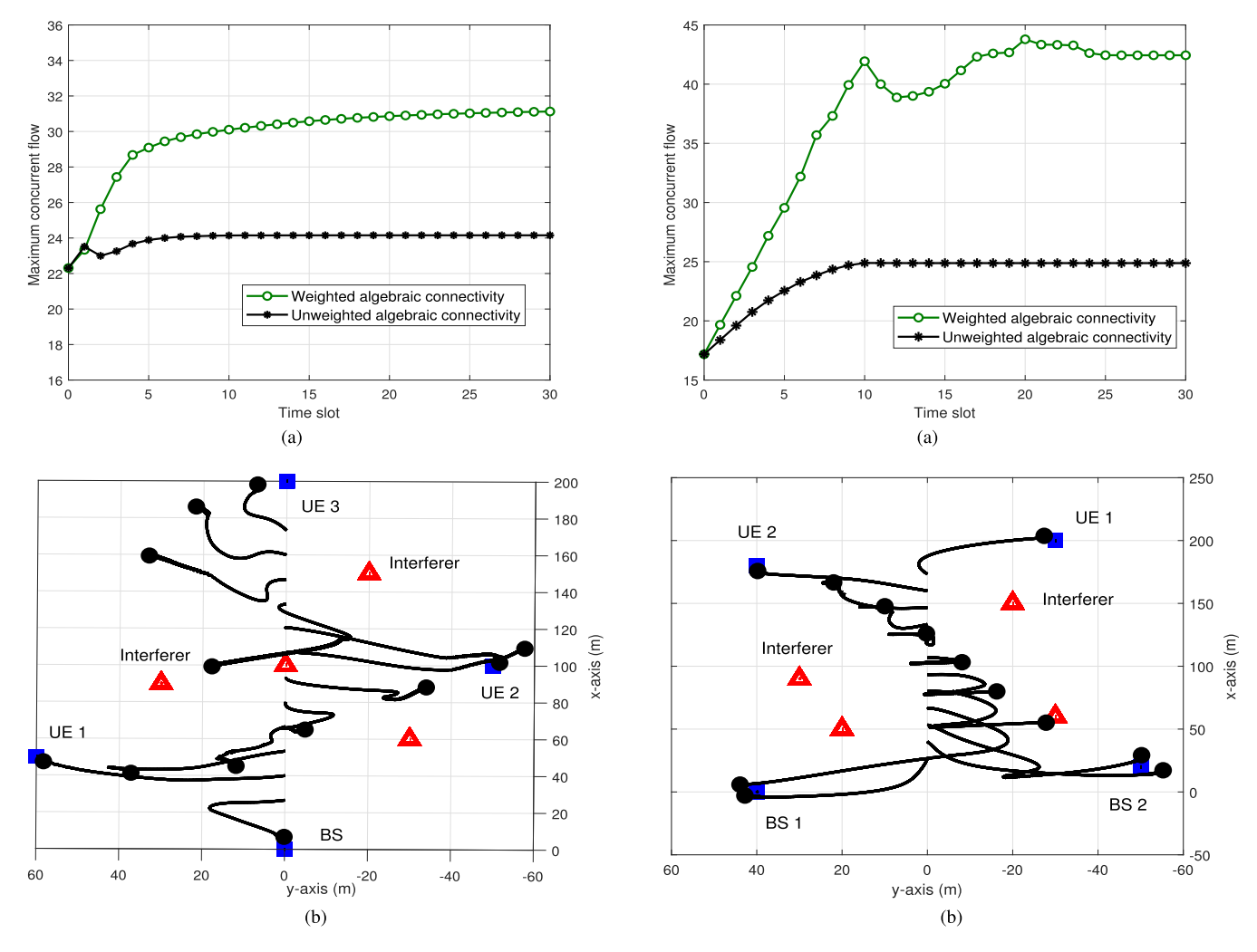


Fig. 7. Performance of the proposed approach for multi-cast scenario (a) Comparison of the throughout of the network for weighted/unweighted Cheeger constant (b) Top view trajectories of the UAVs.

Fig. 8. Performance of the proposed approach for multi-unicast case (a) Comparison of the throughout of the network for weighted/unweighted Cheeger constant (b) Top view trajectories of the UAVs.

3) Interference Avoidance Capability: In Fig. 5, we depict the maximum flow against the interference threshold I^{\max} for the UE altitude of $h^{\rm UE} = 25 \, \rm m$, which may well represent a low-flying UAV as the desired UE. We consider 8 UAVs and one interferer on the ground. We observe that when the relaying UAVs trajectories are optimized in 2D space only (i.e., in xy-, xz-, or yz- planes), their performances are always inferior to that of the 3D trajectory optimization. It can be seen that if the interferer transmit power is optimized, the UAV network performance can be further improved since the interferer does not generate stronger interference at UAV network beyond satisfying the QoS constraint. Moreover, in the case of non-cooperation it may not be practical for UAVs to obtain the positions of unintentional interferers perfectly. Thus, we provide the performance for a 10 percent localization error with confidence interval of 95%. As can be seen, although the maximum flow of the UAV degrades due to imperfect localization, it still provides satisfying performance compared to the 2D trajectory design. One other aspect of comparison between 2D and 3D trajectory design is energy consumption for traversing the trajectory. It can be seen that in case

of 3D trajectory design the UAVs traverse longer trajectories ending up with better performance in improving the maximum flow of the network, while it increases the moving energy consumption.

4) Impact of the UE Altitude: In this section, our goal is to evaluate the impact of the height of the UE on maximum flow of the UAV network. To do so, we assume that the UE (destination) can also move in the direction z-axis. We consider 10 interferers and 8 UAVs in this scenario. In Fig. 6a, we present the maximum flow along with increasing the height of the UE. Interestingly, maximum flow improves with increasing altitude until $h^{\rm UE} = 110 \,\mathrm{m}$ and decreases after that. This implies that there is an optimal height for the location of the UE that can be achieved. To illustrate this situation, we depict the 3D trajectories of all the 8 UAVs in Fig. 6b for the UE altitudes of $h^{\rm UE} = \{15, 110\}$ m. Further increasing the altitude beyond $h^{\rm UE}=110{\rm m}$ may decrease the maximum flow due to the increasing path loss to the source, which becomes more dominant over the interference from interferers (even though the interference is also decreasing due to the increasing distance).

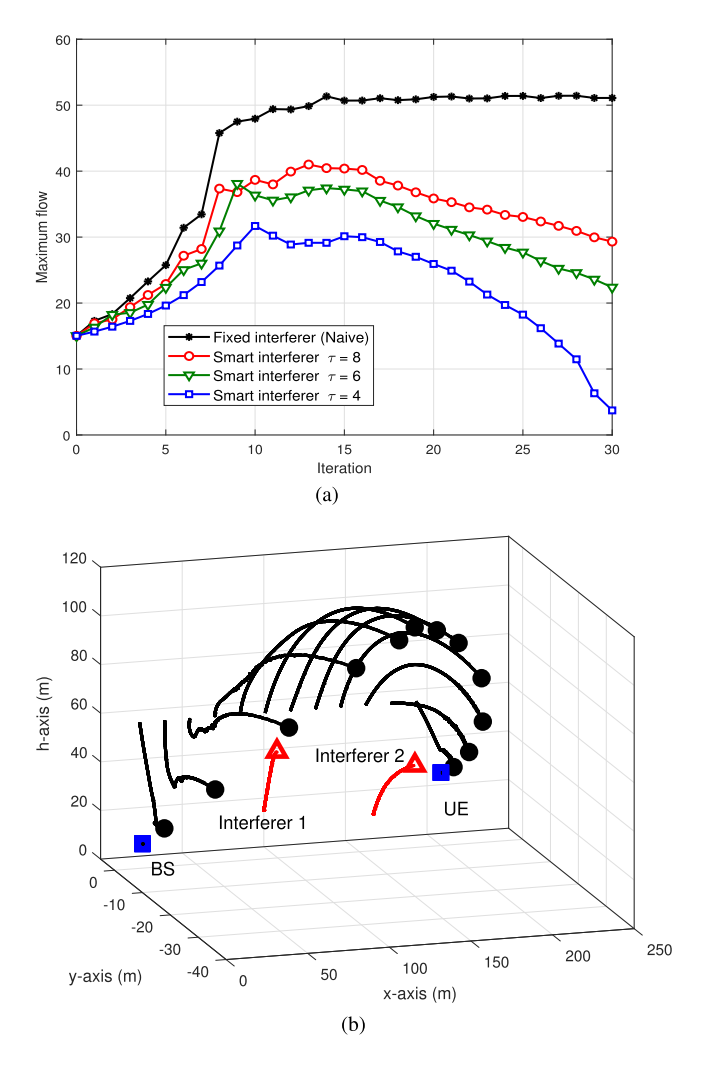
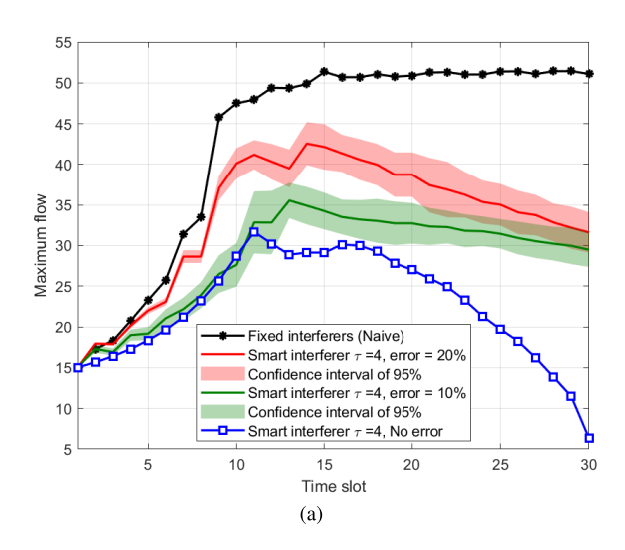


Fig. 9. (a) The maximum flow of the UAV network with smart interferer, where decreasing τ corresponds to a smarter interferer. (b) 3D trajectories of relaying UAVs and the smart interferers (τ = 2).

5) Multiple UEs: The proposed approach can be extended to the case of multiple UEs. In this scenario, we consider both multi-cast and multi-cast scenarios. For the case of multicast scenario, we consider 1 BS, 3 UEs and 4 interferers. The BS transmits the flow to multiple UEs with the help of 12 UAV relays. Here, we assume $\beta = P_{\text{max}}/1000$ as our power allocation quantization step. In Fig. 7a and Fig. 7b, we show the maximum concurrent flow of the network with weighted/unweighted algebraic connectivity and top view of the trajectories of the UAVs, respectively. The trajectories are formed in a way that UAVs try to evade the interferers and get close to the UEs and BS as much as possible. It is observed that the proposed method is effective in the multi-cast case as well. For the multi-unicast case, we consider 2 BSs and 2 UEs. Each BS is associated with its own UE for data transmission, in the presence of 4 interferers. In Fig. 8a and Fig. 8b, we again show network concurrent flow and top view trajectories of the UAVs, respectively. As shown, the weighted algebraic connectivity based trajectory design can improve the flow significantly compared to that of the unweighted case.



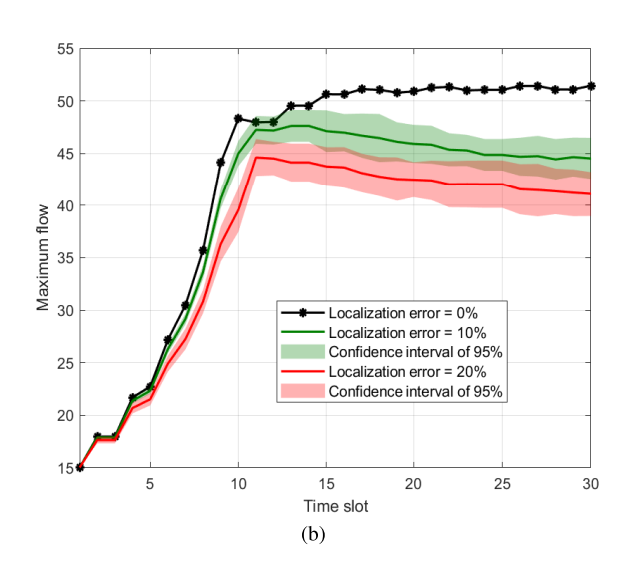


Fig. 10. (a) The maximum data flow of the UAV network considering different localization errors on the smart jammer's side. (b) The maximum flow of the UAV network considering different localization errors on the UAVs' side.

B. Smart Interferer

We finally consider a scenario involving two smart interferers, which are smart UAVs, as discussed in Section IV-B. In order to evaluate the performance, we assume 12 UAVs and a UE at a height of 40 m (i.e., another UAV). The smart interferers start their movement at an initial point and chase relaying UAVs. Note that we control the smartness of the interferer with the parameter τ , which denotes the ability of the interferer to adjust its 3D location. The value of au controls the time interferer needed to find its direction towards the "best" 3D location at. When $\tau = 1$, the jammer can with same speed of the legitimate UAVs. Considering a certain amount of time that the smart interferer needs to estimate the UAV-relaying parameters so as to decide the best strategy, we assume $\tau > 1$ to have a realistic scenario. We also depict the data flow performance of the UAV-assisted network in Fig. 9a for smart interferers with $\tau \in \{4, 6, 8\}$ and the naive

interferers which are not adjusting their locations. We observe that the maximum flow performance generally degrades as smart interferers become more capable in adjusting their locations (i.e., smaller τ). In Fig. 9b, we depict the UAVs trajectories in 3D. We observe that while smart interferers are chasing the UAVs to decrease the data flow, the relaying UAVs adjust their locations to get away from the smart interferers.

C. Localization Error

In this part, we evaluate the performance of the UAV network in both cases of intentional and unintentional interferers with localization errors in UAV network side and also interferers side. In Fig. 10a, the performance of the UAV network is depicted with different localization errors on the jammer's side. It can be observed that a larger localization error at the jammer grants more vantage to the UAV network. On the other hand, the perfect jammer localization can be challenging for the UAVs as well. As can be seen in Fig. 10b, the maximum flow of the UAV network decreases with the increase of localization error as expected. In the above figures, we have shown the results with confidence interval of 95 percent (where the location error is assumed to be uniform) around the mean curve averaged over 1000 realizations.

VII. CONCLUSION

In this paper, we have considered the joint power and 3D trajectory design for a UAV-assisted relay network in the presence of a primary network. The solution for 3D trajectory design and power allocation is proposed based on spectral graph theory and convex optimization. We approached the problem for both unintentional and smart interferers perspectives. We also extended our work to the multiple UE setting. Simulation results show the effectiveness of the proposed algorithm in improving the maximum flow and interference mitigation. In particular, we have shown that the proposed 3D trajectory design can increase the UAV network maximum flow significantly compared to the 2D trajectory design while satisfying the interference constraint on the primary network. Moreover, we have shown that there exists an optimal altitude for the UE as a UAV that maximizes the flow of the UAV network. We also observed that the UAVs can reconfigure their locations to evade the smart interferer, while smart interferers chase the UAVs so as to decrease the maximum flow of the network by increasing the interference resulted from decreasing the path loss effect.

REFERENCES

- [1] A. Rahmati *et al.*, "Interference avoidance in UAV-assisted networks: Joint 3D trajectory design and power allocation," in *Proc. IEEE Global Commun. Conf. (GLOBECOM)*, Big Island, HI, USA, Dec. 2019, pp. 1–6.
- [2] G. Ding, Q. Wu, L. Zhang, Y. Lin, T. A. Tsiftsis, and Y.-D. Yao, "An amateur drone surveillance system based on the cognitive Internet of Things," *IEEE Commun. Mag.*, vol. 56, no. 1, pp. 29–35, Jan. 2018.
- [3] S. Hosseinalipour, A. Rahmati, D. Y. Eun, and H. Dai, "Energy-aware stochastic UAV-assisted surveillance," *IEEE Trans. Wireless Commun.*, vol. 20, no. 5, pp. 2820–2837, May 2021.
- [4] Y. Zeng and R. Zhang, "Energy-efficient UAV communication with trajectory optimization," *IEEE Trans. Wireless Commun.*, vol. 16, no. 6, pp. 3747–3760, Jun. 2017.

- [5] M. Mozaffari, A. T. Z. Kasgari, W. Saad, M. Bennis, and M. Debbah, "Beyond 5G with UAVs: Foundations of a 3D wireless cellular network," *IEEE Trans. Wireless Commun.*, vol. 18, no. 1, pp. 357–372, 2019.
- [6] A. Rahmati, Y. Yapici, N. Rupasinghe, I. Guvenc, H. Dai, and A. Bhuyan, "Energy efficiency of RSMA and NOMA in cellularconnected mmWave UAV networks," in *Proc. IEEE Int. Conf. Commun.* Workshops (ICC Workshops), Shanghai, China, May 2019, pp. 1–6.
- [7] Y. Zeng, J. Lyu, and R. Zhang, "Cellular-connected UAV: Potential, challenges, and promising technologies," *IEEE Wireless Commun.*, vol. 26, no. 1, pp. 120–127, Feb. 2019.
- [8] S. Sekander, H. Tabassum, and E. Hossain, "Multi-tier drone architecture for 5G/B5G cellular networks: Challenges, trends, and prospects," *IEEE Commun. Mag.*, vol. 56, no. 3, pp. 96–103, Mar. 2018.
- [9] M. Younis and K. Akkaya, "Strategies and techniques for node placement in wireless sensor networks: A survey," Ad Hoc Netw., vol. 6, no. 4, pp. 621–655, 2008.
- [10] P. Zhan, K. Yu, and A. L. Swindlehurst, "Wireless relay communications using an unmanned aerial vehicle," in *Proc. IEEE 7th Workshop Signal Process. Adv. Wireless Commun.*, Cannes, France, Jul. 2006, pp. 1–5.
- [11] Q. Wang, Z. Chen, W. Mei, and J. Fang, "Improving physical layer security using UAV-enabled mobile relaying," *IEEE Wireless Commun. Lett.*, vol. 6, no. 3, pp. 310–313, Jun. 2017.
- [12] U. Challita and W. Saad, "Network formation in the sky: Unmanned aerial vehicles for multi-hop wireless backhauling," in *Proc. IEEE Global Commun. Conf. (GLOBECOM)*, Singapore, Dec. 2017, pp. 1–6.
- [13] Y. Chen, N. Zhao, Z. Ding, and M.-S. Alouini, "Multiple UAVs as relays: Multi-hop single link versus multiple dual-hop links," *IEEE Trans. Wireless Commun.*, vol. 17, no. 9, pp. 6348–6359, Sep. 2018.
- [14] S. Hosseinalipour, A. Rahmati, and H. Dai, "Interference avoidance position planning in UAV-assisted wireless communication," in *Proc.* IEEE Int. Conf. Commun. (ICC), Shanghai, China, May 2019, pp. 1–6.
- [15] O. J. Faqir, Y. Nie, E. C. Kerrigan, and D. Gündüz, "Energy-efficient communication in mobile aerial relay-assisted networks using predictive control," *IFAC-PapersOnLine*, vol. 51, no. 20, pp. 197–202, 2018.
- [16] Y. Chen, W. Feng, and G. Zheng, "Optimum placement of UAV as relays," *IEEE Commun. Lett.*, vol. 22, no. 2, pp. 248–251, Feb. 2018.
- [17] S. Zhang, H. Zhang, Q. He, K. Bian, and L. Song, "Joint trajectory and power optimization for UAV relay networks," *IEEE Commun. Lett.*, vol. 22, no. 1, pp. 161–164, Oct. 2017.
- [18] Y. Zeng et al., "Throughput maximization for UAV-enabled mobile relaying systems," *IEEE Trans. Commun.*, vol. 64, no. 12, pp. 4983–4996, Dec. 2016.
- [19] F. Ono, H. Ochiai, and R. Miura, "A wireless relay network based on unmanned aircraft system with rate optimization," *IEEE Trans. Wireless Commun.*, vol. 15, no. 11, pp. 7699–7708, Nov. 2016.
- [20] J. Chen and D. Gesbert, "Efficient local map search algorithms for the placement of flying relays," *IEEE Trans. Wireless Commun.*, vol. 19, no. 2, pp. 1305–1319, Feb. 2020.
- [21] M. M. U. Chowdhury, S. J. Maeng, E. Bulut, and I. Guvenc, "Effects of 3D antenna radiation and two-hop relaying on optimal UAV trajectory in cellular networks," in *Proc. IEEE Aerosp. Conf.*, Big Sky, ID, USA, Mar. 2019, pp. 1–11.
- [22] S. Hosseinalipour, A. Rahmati, and H. Dai, "Interference avoidance position planning in dual-hop and multi-hop UAV relay networks," *IEEE Trans. Wireless Commun.*, vol. 19, no. 11, pp. 7033–7048, Nov. 2020.
- [23] J. Chen and D. Gesbert, "Optimal positioning of flying relays for wireless networks: A LOS map approach," in *Proc. IEEE Int. Conf.* Commun. (ICC), May 2017, pp. 1–6.
- [24] G. Zhang, H. Yan, Y. Zeng, M. Cui, and Y. Liu, "Trajectory optimization and power allocation for multi-hop UAV relaying communications," *IEEE Access*, vol. 6, pp. 48566–48576, 2018.
- [25] X. Jiang, Z. Wu, Z. Yin, W. Yang, and Z. Yang, "Trajectory and communication design for UAV-relayed wireless networks," *IEEE Wireless Commun. Lett.*, vol. 8, no. 6, pp. 1600–1603, Dec. 2019.
- [26] J. Fan, M. Cui, G. Zhang, and Y. Chen, "Throughput improvement for multi-hop UAV relaying," *IEEE Access*, vol. 7, pp. 147732–147742, 2019
- [27] S. Eom, H. Lee, J. Park, and I. Lee, "UAV-aided two-way mobile relaying systems," *IEEE Commun. Lett.*, vol. 24, no. 2, pp. 438–442, Feb. 2020.
- [28] M.-C. Mah, H.-S. Lim, and A. W.-C. Tan, "UAV relay flight path planning in the presence of jamming signal," *IEEE Access*, vol. 7, pp. 40913–40924, 2019.
- [29] J. Miao and Z. Zheng, "Cooperative jamming for secure UAV-enabled mobile relay system," *IEEE Access*, vol. 8, pp. 48943–48957, 2020.

- [30] N. Zhao et al., "Caching UAV assisted secure transmission in hyperdense networks based on interference alignment," IEEE Trans. Commun., vol. 66, no. 5, pp. 2281–2294, May 2018.
- [31] X. Liu *et al.*, "Transceiver design and multihop D2D for UAV IoT coverage in disasters," *IEEE Internet Things J.*, vol. 6, no. 2, pp. 1803–1815, Apr. 2018.
- [32] S. Zhang, H. Zhang, B. Di, and L. Song, "Cellular UAV-to-X communications: Design and optimization for multi-UAV networks," *IEEE Trans. Wireless Commun.*, vol. 18, no. 2, pp. 1346–1359, Jan. 2019.
- [33] Y. Che, Y. Lai, S. Luo, K. Wu, and L. Duan, "UAV-aided information and energy transmissions for cognitive and sustainable 5G networks," *IEEE Trans. Wireless Commun.*, vol. 20, no. 3, pp. 1668–1683, Mar. 2021.
- [34] Y. Han, L. Liu, L. Duan, and R. Zhang, "Towards reliable UAV swarm communication in D2D-enhanced cellular networks," *IEEE Trans. Wireless Commun.*, vol. 20, no. 3, pp. 1567–1581, Mar. 2020.
 [35] S. Yin, Y. Zhao, and L. Li, "UAV-assisted cooperative communications
- [35] S. Yin, Y. Zhao, and L. Li, "UAV-assisted cooperative communications with time-sharing SWIPT," in *Proc. IEEE Int. Conf. Commun. (ICC)*, May 2018, pp. 1–6.
- [36] M. Tavana, A. Rahmati, V. Shah-Mansouri, and B. Maham, "Cooperative sensing with joint energy and correlation detection in cognitive radio networks," *IEEE Commun. Lett.*, vol. 21, no. 1, pp. 132–135, Jan. 2017.
- [37] A. Al-Hourani, S. Kandeepan, and A. Jamalipour, "Modeling air-to-ground path loss for low altitude platforms in urban environments," in *Proc. IEEE Global Commun. Conf. (GLOBECOM)*, Austin, TX, USA, Dec. 2014, pp. 2898–2904.
- [38] M. Mozaffari, W. Saad, M. Bennis, and M. Debbah, "Mobile unmanned aerial vehicles (UAVs) for energy-efficient Internet of Things communications," *IEEE Trans. Wireless Commun.*, vol. 16, no. 11, pp. 7574–7589, Nov. 2017.
- [39] M. Mozaffari, W. Saad, M. Bennis, and M. Debbah, "Optimal transport theory for power-efficient deployment of unmanned aerial vehicles," in *Proc. IEEE Int. Conf. Commun. (ICC)*, May 2016, pp. 1–6.
- [40] J. Schroeder, A. Guedes, and E. P. Duarte, Jr., "Computing the minimum cut and maximum flow of undirected graphs," Federal Univ. Paraná, Curitiba, Brazil, Tech. Rep. RT-DINF 003/2004, 2004.
- [41] R. Madan, D. Shah, and O. Leveque, "Product multicommodity flow in wireless networks," *IEEE Trans. Inf. Theory*, vol. 54, no. 4, pp. 1460–1476, Apr. 2008.
- [42] R. Weibel and R. J. Hansman, "Safety considerations for operation of different classes of UAVs in the NAS," in *Proc. AIAA 4th Aviation Technol.*, *Integr. Operations (ATIO) Forum*, 2004, p. 6244.
- [43] J. C. Bezdek and R. J. Hathaway, "Some notes on alternating optimization," in *Proc. AFSS Int. Conf. Fuzzy Sys.* Berlin, Germany: Springer, 2002, pp. 288–300.
- [44] L. R. Ford, Jr., and D. R. Fulkerson, Flows in Networks. Princeton, NJ, USA: Princeton Univ. Press, 2015.
- [45] X. He, H. Dai, and P. Ning, "Dynamic adaptive anti-jamming via controlled mobility," *IEEE Trans. Wireless Commun.*, vol. 13, no. 8, pp. 4374–4388, Aug. 2014.
- [46] F. R. Chung and F. C. Graham, *Spectral Graph Theory*. Fresno, CA, USA: American Mathematical Soc., 1997, no. 92.
- [47] A. Bertrand and M. Moonen, "Distributed computation of the Fiedler vector with application to topology inference in ad hoc networks," *Signal Process.*, vol. 93, no. 5, pp. 1106–1117, May 2013.
- [48] M. Grant and S. Boyd, "CVX: MATLAB software for disciplined convex programming, version 2.1," Tech. Rep., 2014.
- [49] M. Chiang, C. W. Tan, D. P. Palomar, D. O'Neill, and D. Julian, "Power control by geometric programming," *IEEE Trans. Wireless Commun.*, vol. 6, no. 7, pp. 2640–2651, 2007, doi: 10.1109/TWC.2007.05960.
- [50] S. Boyd and L. Vandenberghe, Convex Optimization. Cambridge, U.K.: Cambridge Univ. Press, 2004.
- [51] A. A. Nasir, D. T. Ngo, X. Zhou, R. A. Kennedy, and S. Durrani, "Joint resource optimization for multicell networks with wireless energy harvesting relays," *IEEE Trans. Veh. Technol.*, vol. 65, no. 8, pp. 6168–6183, Aug. 2016.
- [52] B. Khamidehi, A. Rahmati, and M. Sabbaghian, "Joint sub-channel assignment and power allocation in heterogeneous networks: An efficient optimization method," *IEEE Commun. Lett.*, vol. 20, no. 12, pp. 2490–2493, Dec. 2016.
- [53] H. H. Kha, H. D. Tuan, and H. H. Nguyen, "Fast global optimal power allocation in wireless networks by local DC programming," *IEEE Trans. Wireless Commun.*, vol. 11, no. 2, pp. 510–515, Dec. 2011.
- [54] S. Ruder, "An overview of gradient descent optimization algorithms," 2016, arXiv:1609.04747. [Online]. Available: https://arxiv.org/abs/1609.04747
- [55] M. Grant, S. Boyd, and Y. Ye, "CVX: MATLAB software for disciplined convex programming," Tech. Rep., 2008.

- [56] A. Khalili, S. Akhlaghi, H. Tabassum, and D. W. K. Ng, "Joint user association and resource allocation in the uplink of heterogeneous networks," *IEEE Wireless Commun. Lett.*, vol. 9, no. 6, pp. 804–808, 2020, doi: 10.1109/LWC.2020.2970696.
- [57] O. Abbasi, H. Yanikomeroglu, A. Ebrahimi, and N. M. Yamchi, "Trajectory design and power allocation for drone-assisted NR-V2X network with dynamic NOMA/OMA," *IEEE Trans. Wireless Commun.*, vol. 19, no. 11, pp. 7153–7168, Nov. 2020.
- [58] N. Mokari, F. Alavi, S. Parsaeefard, and T. Le-Ngoc, "Limited-feedback resource allocation in heterogeneous cellular networks," *IEEE Trans.* Veh. Technol., vol. 65, no. 4, pp. 2509–2521, Apr. 2015.
- [59] V. Y. Pan and Z. Q. Chen, "The complexity of the matrix eigenproblem," in *Proc. 31st Annu. ACM Symp. Theory Comput. (STOC)*, 1999, pp. 507–516.
- [60] T. Leighton and S. Rao, "Multicommodity max-flow min-cut theorems and their use in designing approximation algorithms," J. ACM, vol. 46, no. 6, pp. 787–832, Nov. 1999.



Ali Rahmati (Member, IEEE) received the B.Sc. degree in electrical engineering from Ferdowsi University of Mashhad, Mashhad, Iran, the M.S. degree in electrical engineering from the University of Tehran, Tehran, Iran, and the Ph.D. degree in electrical engineering from the Department of Electrical and Computer Engineering, North Carolina State University, Raleigh, NC, USA. He is currently a Senior Engineer with Qualcomm. His research interests mainly include applications of game theory, optimization, and machine learning in wireless communication networks.



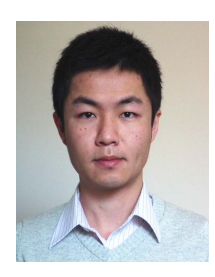
Seyyedali Hosseinalipour (Member, IEEE) received the B.S. degree in electrical engineering from Amirkabir University of Technology, Tehran, Iran, in 2015, and the M.S. and Ph.D. degrees in electrical engineering from North Carolina State University, NC, USA, in 2017 and 2020, respectively. He is currently a Postdoctoral Researcher with Purdue University, IN, USA. His research interests include the analysis of modern wireless networks and communication systems, distributed machine learning, and network

optimization. He was a recipient of ECE Doctoral Scholar of the Year Award in 2020 and ECE Distinguished Dissertation Award in 2021 at North Carolina State University. He served as a TPC Member for Edge Machine Learning for 5G Mobile Networks and Beyond (EdgeLearn5G), held in conjunction with IEEE ICC 2021; and a Program Committee Member for Edge Computing and IoT, IEEE MSN. He has served as the TPC Co-Chair for The First International Workshop on Distributed Machine Learning and Fog Networks (FogML), held in conjunction with IEEE INFOCOM 2021; and the 2nd Workshop on Edge Learning Over 5G Mobile Networks and Beyond (EL5GMNB), held in conjunction with IEEE GLOBECOM 2021.



Yavuz Yapıcı (Senior Member, IEEE) received the B.S. and M.S. degrees in electrical and electronics engineering from Bilkent University, Ankara, Turkey, in 2002 and 2005, respectively, and the Ph.D. degree in electrical and electronics engineering from Middle East Technical University, Ankara, in 2011. He is currently a Senior Staff Engineer with Qualcomm. He was previously an Assistant Professor with the Department of Electrical Engineering, University of South Carolina, Columbia, SC, USA. His research interests include

the next-generation wireless communications technologies with a particular emphasis on spectrum/energy-efficient and secure millimeter-wave communications.



Xiaofan He (Member, IEEE) received the B.S. degree in electronics and information engineering from the Huazhong University of Science and Technology, Wuhan, China, in 2008, the M.S. degree in electrical and computer engineering from McMaster University, Hamilton, ON, Canada, in 2011, and the Ph.D. degree in electrical and computer engineering from North Carolina State University, Raleigh, NC, USA, in 2015. He was a Tenure-Track Assistant Professor of electrical engineering with Lamar University, TX, USA, from 2016 to 2018. He moved

back to his hometown Wuhan in 2019, and currently a Faculty Member with the Electronic Information School, Wuhan University, Wuhan. His research interests are in the general areas of wireless communications and networking. His current research mainly focuses on edge computing and the associated optimization, reinforcement learning, and statistical analysis issues. He received the Exemplary Reviewer Award of IEEE TRANSACTIONS ON COMMUNICATIONS in 2014 and 2015, and the Distinguished Member of Technical Program Committee Award of IEEE INFOCOM in 2018. He is currently serving as an Associate Editor for IEEE ACCESS.



Ismail Güvenç (Fellow, IEEE) received the Ph.D. degree in electrical engineering from the University of South Florida in 2006.

He was with Mitsubishi Electric Research Labs in 2005, DOCOMO Innovations from 2006 to 2012, and Florida International University from 2012 to 2016. From 2016 to 2020, he was an Associate Professor, and since 2020, he has been a Professor with the Department of Electrical and Computer Engineering, North Carolina State University. He has published more than 300 conference/journal arti-

cles and book chapters, and several standardization contributions. He has coauthored/co-edited four books. He is an inventor/co-inventor of some 30 U.S. patents. His recent research interests include 5G wireless systems, communications and networking with drones, and heterogeneous wireless networks. He is a Senior Member of the National Academy of Inventors. He was a recipient of USF Outstanding Dissertation Award in 2006, Ralph E. Powe Junior Faculty Enhancement Award in 2014, NSF CAREER Award in 2015, FIU College of Engineering Faculty Research Award in 2016, and NCSU ECE R. Ray Bennett Faculty Fellow Award in 2019. He has served as an Editor for IEEE COMMUNICATIONS LETTERS from 2010 to 2015 and IEEE WIRELESS COMMUNICATIONS LETTERS from 2011 to 2016. He has been serving as an Editor for IEEE TRANSACTIONS ON WIRELESS COMMUNICATIONS since 2016. He has served as a guest editor for several other journals.



Huaiyu Dai (Fellow, IEEE) received the B.E. and M.S. degrees in electrical engineering from Tsinghua University, Beijing, China, in 1996 and 1998, respectively, and the Ph.D. degree in electrical engineering from Princeton University, Princeton, NJ, in 2002.

He was with Bell Labs, Lucent Technologies, Holmdel, NJ, in summer 2000, and with AT&T Labs-Research, Middletown, NJ, in summer 2001. He is currently a Professor of electrical and computer engineering with NC State University, Raleigh,

holding the title of University Faculty Scholar. His research interests are in the general areas of communications, signal processing, networking, and computing. His current research focuses on machine learning and artificial intelligence for communications and networking, multilayer and interdependent networks, dynamic spectrum access and sharing, as well as security and privacy issues in the above systems. He has served as an Editor for IEEE TRANSACTIONS ON COMMUNICATIONS, IEEE TRANSACTIONS ON SIGNAL PROCESSING, and IEEE TRANSACTIONS ON WIRELESS COMMUNICATIONS. He is currently an Area Editor in charge of wireless communications for IEEE TRANSACTIONS ON COMMUNICATIONS, and a member of the Executive Editorial Committee for IEEE TRANSACTIONS ON WIRELESS COMMUNICATIONS. He was a corecipient of best paper awards at the 2010 IEEE International Conference on Mobile Ad-hoc and Sensor Systems (MASS 2010), the 2016 IEEE INFOCOM BIGSECURITY Workshop, and the 2017 IEEE International Conference on Communications (ICC 2017).



Arupjyoti (Arup) Bhuyan (Senior Member, IEEE) received the Ph.D. degree in engineering and applied sciences from Yale University. He is currently a Wireless Researcher with Idaho National Laboratory (INL) and the Technical Director of INL Wireless Security Institute. The focus of his research is on secure implementation of future generations of wireless communications with scientific exploration and engineering innovations across the fields of wireless technology, cybersecurity, and computational science. His specific goals are to assure

communications among critical infrastructure systems supporting control of the electric grid, emergency response, and nationwide unmanned aerial systems. He has extensive industry experience in wireless communications from his work before he joined INL in October 2015.